

# Preparation and characterization of 1,3,2-dithiazolidine and 1,4-dithia-7-azabicyclo[2.2.1]heptane cations, and a mechanistic study of the cycloaddition reactions of alkenes with SNS<sup>+</sup>†

Wendell V. F. Brooks, Scott Brownridge, Jack Passmore,\* Melbourne J. Schriver and Xiaoping Sun

Department of Chemistry, University of New Brunswick, Fredericton, N.B., E3B 6E2, Canada

The cation SNS<sup>+</sup> (as the AsF<sub>6</sub><sup>-</sup> salt) underwent quantitative concerted symmetry-allowed cycloaddition reactions with alkenes [C<sub>2</sub>H<sub>4</sub>, *trans*- and *cis*-MeHCCHMe, H<sub>2</sub>CCMe<sub>2</sub>, MeHCCH<sub>2</sub>, Me<sub>2</sub>CCMe<sub>2</sub> and norbornene (bicyclo[2.2.1]hept-2-ene)] to give 1,3,2-dithiazolidine cations **1**, which in a second quantitative concerted symmetry-allowed cycloaddition reaction with another alkene molecule gave 1,4-dithia-7-azabicyclo[2.2.1]heptane cations **2** (with the exception of Me<sub>2</sub>CCMe<sub>2</sub>). The cycloadducts were characterized by elemental analyses and IR and NMR (<sup>1</sup>H, <sup>13</sup>C, <sup>14</sup>N) spectroscopies. The vibrational spectra were assigned with the aid of frequencies obtained by *ab initio* (RHF/6-31G\*) calculations. When alkene = C<sub>2</sub>H<sub>4</sub> the calculated geometry of **2** was in good agreement with that obtained from its crystal structure reported previously; that of **1** correlates well with the experimental data (IR, Fourier-transform Raman, NMR). Kinetic studies showed that the rate constants of the first cycloaddition of SNS<sup>+</sup> to C<sub>2</sub>H<sub>4</sub> are comparable with those of nitrile and alkyne cycloadditions, indicating that the cycloaddition proceeds *via* the interaction of the highest occupied molecular orbital of the alkene and the lowest unoccupied one of SNS<sup>+</sup> as was previously observed for various nitriles and alkynes. The second cycloaddition leads to stereospecific **2**, except for H<sub>2</sub>CCHMe. Contrary to the prediction of a simple frontier molecular model, the rate of the second cycloaddition was faster than the first for C<sub>2</sub>H<sub>4</sub>, *cis*-MeHCCHMe, and H<sub>2</sub>CCMe<sub>2</sub> and strongly dependent on the steric activity of the alkene. It is proposed that the second cycloaddition likely occurs *via* a concerted and synchronous pathway.

In the last few years an extensive chemistry of the cation SNS<sup>+</sup> (as SNS<sup>+</sup>AsF<sub>6</sub><sup>-</sup>) has been developed.<sup>1</sup> One of the most remarkable features is the ease with which it undergoes quantitative concerted symmetry-allowed cycloaddition reactions with a wide variety of π bonds (*i.e.* C≡N,<sup>2a,b,d,e,g,i</sup> C≡C,<sup>2a,b,d,e,g</sup> SN<sup>+</sup>,<sup>2c</sup> C≡P,<sup>2h</sup> and reported for C=N,<sup>2f</sup> P=N,<sup>2f</sup> P=P<sup>2f</sup> and N=N<sup>2f</sup> but experimental details have not yet been published). This is in contrast to the cycloadditions of neutral S–N compounds which generally only occur with strained alkenes (*e.g.* norbornene, bicyclo[2.2.1]hept-2-ene),<sup>3</sup> or react with unsaturated organic species under forcing conditions to give complex mixtures.<sup>4</sup> However, 1,3,2,4,6-dithiatiazines have been shown to form adducts with unstrained alkenes, attributed to their strongly antiaromatic 8π electron structure.<sup>5</sup> Oakley and co-workers<sup>3</sup> demonstrated that, in general, cycloaddition reactions of neutral S–N compounds with strained alkenes occur *via* a reverse demand process with the primary interaction from the highest occupied molecular orbital (HOMO) of the alkene into the lowest unoccupied molecular orbital (LUMO) of the S–N species. We predicted that the rate of reaction between SNS<sup>+</sup> and a series of π-bonded molecules would be fastest for reaction with π bonds of lowest ionization energy. This was shown to be the case for a wide variety of alkynes and nitriles with a qualitatively linear correlation for all the data and quantitatively linear correlation for the nitriles alone.<sup>2d</sup> The cation SNS<sup>+</sup> in all cases acts simply as a Lewis acid (electron acceptor) and the alkynes and nitriles as Lewis bases (electron donor). An exploration of the chemistry of SNS<sup>+</sup> with alkenes was therefore of interest. In a preliminary communication we reported that SNS<sup>+</sup> did undergo the anticipated symmetry-allowed cycloaddition reactions with unstrained alkenes but in addition a second



	<b>R<sub>2</sub>CCR<sub>2</sub></b>
<b>1a, 2a</b>	H <sub>2</sub> CCH <sub>2</sub>
<b>1a, 2b</b>	<i>trans</i> -MeHCCHMe
<b>1c, 2c</b>	<i>cis</i> -MeHCCHMe
<b>1d, 2d</b>	H <sub>2</sub> CCMe <sub>2</sub>
<b>1e</b>	Me <sub>2</sub> CCMe <sub>2</sub>
<b>2f</b>	alkene = H <sub>2</sub> CCH <sub>2</sub> , alkene' = <i>trans</i> -MeHCCHMe
<b>1g, 2g</b>	norbornene (C <sub>7</sub> H <sub>10</sub> )

cycloaddition of alkene to the initial 1:1 cycloadduct was observed.<sup>6</sup> In this paper we give a full account of our synthetic investigations<sup>2g</sup> and an investigation of the reaction pathways based on kinetic studies<sup>2i</sup> and a frontier molecular orbital (FMO) model.

## Experimental

### Instrumentation, reaction vessels and starting materials

Unless otherwise specified, reagents and techniques used were as described.<sup>2d,e,7</sup> The purity of the reagents [C<sub>2</sub>H<sub>4</sub>, *trans*- and *cis*-MeHCCHMe, H<sub>2</sub>CCMe<sub>2</sub>, Me<sub>2</sub>CCMe<sub>2</sub> and C<sub>7</sub>H<sub>10</sub> (Aldrich)] were established by their IR and NMR (<sup>1</sup>H and <sup>13</sup>C) spectra. The compound SNSAsF<sub>6</sub> was prepared as reported.<sup>8</sup> The NMR (<sup>1</sup>H, <sup>13</sup>C and <sup>14</sup>N) spectra were obtained as previously reported<sup>2d,e</sup> using a Varian XL-200 MHz spectrometer, IR spectra as Nujol mulls with KBr plates in the region 4000–200 cm<sup>-1</sup> using a Perkin-Elmer 683 spectrometer. The Fourier-transform (FT) Raman spectrum of the AsF<sub>6</sub><sup>-</sup> salt of cation **1a** (alkene = H<sub>2</sub>CCH<sub>2</sub>) was obtained at room temperature as previously described<sup>7</sup> using a Bruker IFS-66

† Supplementary data available (No. SUP 57125, 51 pp.): IR and NMR spectra, theoretical vibrational frequency calculations. See Instructions for Authors, *J. Chem. Soc., Dalton Trans.*, 1996, Issue 1.

Non-SI units employed: eV ≈ 1.60 × 10<sup>-19</sup> J, E<sub>h</sub> ≈ 4.36 × 10<sup>-18</sup> J.

FT-IR spectrometer equipped with an FT-Raman accessory (Bruker FRA-106) and an Nd-YAG laser (emission wavelength 1064 nm, maximum laser power 300 mW). All reactions were performed in two-bulbed reaction vessels (*ca.* 20 cm<sup>3</sup>), incorporating a sintered coarse or medium glass frit and J. Young Teflon-in-glass valves.

#### Reactions of SNSAsF<sub>6</sub> with alkenes [C<sub>2</sub>H<sub>4</sub>, *trans*-MeHCCHMe, norbornene (C<sub>7</sub>H<sub>10</sub>) and H<sub>2</sub>CCHMe] in SO<sub>2</sub> solution (1:1 and 1:2 stoichiometries)

The volatile alkenes C<sub>2</sub>H<sub>4</sub>, *trans*-MeHCCHMe and H<sub>2</sub>CCHMe and SO<sub>2</sub> were condensed onto SNSAsF<sub>6</sub> at -196 °C, and the reactants warmed to room temperature. The non-volatile C<sub>7</sub>H<sub>10</sub> was dissolved in SO<sub>2</sub>, and the solution poured onto SNSAsF<sub>6</sub> at room temperature. In all cases the solutions immediately became clear yellow. For the 1:1 reactions the solutions were then poured into the second bulb of the vessel and sealed off by closing the second valve. The contents were then maintained at 60 °C for 48 h over which time they turned bright yellow. The 1:2 reactions were stirred for 1 h at room temperature, giving colourless solutions. The volatile materials were removed by evacuation to give poorly crystalline yellow and colourless solids for the 1:1 and 1:2 reactions respectively. Solutions of the alkenes (C<sub>2</sub>H<sub>4</sub>, *trans*-MeHCCHMe and C<sub>7</sub>H<sub>10</sub>) in liquid SO<sub>2</sub> were observed to precipitate white solids with time (6 h to 1 d). However, the formation of a white precipitate was not observed in the reactions of SNS<sup>+</sup> with C<sub>2</sub>H<sub>4</sub>, *trans*-MeHCCHMe, C<sub>7</sub>H<sub>10</sub> and H<sub>2</sub>CCHMe; presumably the unsaturated species reacted much faster with SNS<sup>+</sup> than with SO<sub>2</sub>. The raw products from the 1:1 and 1:2 reactions were redissolved in fresh SO<sub>2</sub>. The solvent was slowly condensed into the second bulb at 10 (for 1:1 reaction products) or at 4 °C (for 1:2 reaction products) and plate-shaped yellow (1:1 reactions) or colourless (1:2 reactions) crystals were produced with the exception of the reaction of SNSAsF<sub>6</sub> with H<sub>2</sub>CCHMe in a 1:2 ratio which gave a brown tar. The 1:1 and 1:2 reaction products were identified as the AsF<sub>6</sub><sup>-</sup> salts of cations **1** (yellow crystals) and **2** (colourless crystals) respectively by elemental analyses (Table 1), IR (Table 2) and NMR spectroscopy (Figs. 1 and 2). The FT-Raman spectrum of the AsF<sub>6</sub><sup>-</sup> salt of **1a** is given in Fig. 4 and in footnote *a* of Table 3. The <sup>1</sup>H NMR (decoupled) and IR (in footnote *g* in Table 1) spectra of **2** (alkene = H<sub>2</sub>CCHMe) were complex, implying the presence of several isomers. Single crystals of the AsF<sub>6</sub><sup>-</sup> salt of **2a** (alkene = H<sub>2</sub>CCH<sub>2</sub>) were obtained, and its structure determined.<sup>6</sup> Crystals of the corresponding salt of **1a** were brittle and unsuitable for structure determination. The salts hydrolysed on exposure of ground samples to moist air [IR 3200–3400 (N–H) and 1200–1400 cm<sup>-1</sup> (S–O)].

#### Reactions of SNSAsF<sub>6</sub> with an excess of Me<sub>2</sub>CCMe<sub>2</sub>

A large excess of Me<sub>2</sub>CCMe<sub>2</sub> (2.49 g, 29.6 mmol) was condensed onto SNSAsF<sub>6</sub> (0.730 g, 2.73 mmol). The solid changed from yellow to brown in 5 min, to red after 1.5 h and finally to brown after stirring at room temperature for 10 h. All the volatiles were then evacuated under dynamic vacuum for more than 20 h, giving a brown tar:  $\tilde{\nu}_{\max}/\text{cm}^{-1}$  2710w, 2680w, 2180vw, 1600w, 1567m, 1493s, 1302vw, 1250w, 1182m, 1154vw, 1115w, 998m, 896m, 815w, 700vw (br) [ $\nu_3(\text{AsF}_6^-)$ ], 565w, 495w, 390vs [ $\nu_4(\text{AsF}_6^-)$ ]. The spectrum has been deposited (see SUP 57125). <sup>19</sup>F NMR (CD<sub>2</sub>Cl<sub>2</sub> solvent, CFCl<sub>3</sub> reference):  $\delta$  -62.4,  $\nu_1 = 1450$  Hz, AsF<sub>6</sub><sup>-</sup>. The <sup>1</sup>H and <sup>13</sup>C NMR data (CD<sub>2</sub>Cl<sub>2</sub> solvent, SiMe<sub>4</sub> reference) are shown in Fig. 1. In addition, there were a group of weak peaks (unknown impurities) at  $\delta$  30–23.5 in the <sup>13</sup>C spectrum. For <sup>1</sup>H NMR the sample was prepared by dissolving the raw product (0.0266 g) in CD<sub>2</sub>Cl<sub>2</sub> (1.15 g) with CH<sub>2</sub>Cl<sub>2</sub> (0.215 mmol) as internal concentration standard, and several weak peaks (unknown

impurities) were observed at  $\delta$  3.4, 1.25, 0.04 and -1.00. The <sup>1</sup>H and <sup>13</sup>C spectra have been deposited. The raw product was estimated to contain 87% of the AsF<sub>6</sub><sup>-</sup> salt of cation **1e** (alkene = Me<sub>2</sub>CCMe<sub>2</sub>) based on the <sup>1</sup>H NMR integrations. A similar reaction of SNSAsF<sub>6</sub> (0.05 mmol) with a large excess of Me<sub>2</sub>CCMe<sub>2</sub> (0.5 mmol) in CH<sub>2</sub>Cl<sub>2</sub> solution gave a product with a similar <sup>1</sup>H NMR spectrum.

#### Reactions of the AsF<sub>6</sub><sup>-</sup> salts of cations **1a** and **1b** (alkene = *trans*-MeHCCHMe) with C<sub>2</sub>H<sub>4</sub>, *trans*-MeHCCHMe and C<sub>2</sub>H<sub>2</sub>

In a series of experiments, the salts of cations **1a** and **1b** were treated in liquid SO<sub>2</sub> with C<sub>2</sub>H<sub>4</sub>, *trans*-MeHCCHMe and C<sub>2</sub>H<sub>2</sub> at room temperature in thick-walled 5 mm NMR tubes, and unless otherwise specified the products were identified *in situ* by <sup>1</sup>H NMR spectroscopy. The colour changes, apparent reaction times and product analyses are given in Table 4.

#### Reactions of the AsF<sub>6</sub><sup>-</sup> salts of cations **2a** and **2g** (alkene = C<sub>7</sub>H<sub>10</sub>) with SNSAsF<sub>6</sub> and C<sub>2</sub>H<sub>2</sub>

In a series of experiments, the salts of cations **2a** and **2g** were treated in liquid SO<sub>2</sub> with SNSAsF<sub>6</sub>. The reaction data, the colour changes and product analyses are given in Table 5.

#### Determination of the order and absolute rate constant of the reaction of SNSAsF<sub>6</sub> with C<sub>2</sub>H<sub>4</sub>

Sulfur dioxide (0.895 g) and C<sub>2</sub>H<sub>4</sub> (0.132 mmol) were successively condensed onto SNSAsF<sub>6</sub> (0.0217 mmol) in a thick-walled 5 mm NMR tube, which was then flame-sealed. The mixture was quickly warmed to room temperature and <sup>1</sup>H NMR spectra were recorded as a function of time. The concentrations of C<sub>2</sub>H<sub>4</sub>, cations **1a** and **2a** at different times were determined from NMR integrations (Fig. 3).

#### Determination of the ratios of the rate constant (*k*<sub>2</sub>) of the second cycloaddition (cation **1** with alkene) to that (*k*<sub>1</sub>) of the first cycloaddition (SNS<sup>+</sup> with alkene) for C<sub>2</sub>H<sub>4</sub>, *cis*-MeHCCHMe and H<sub>2</sub>CCMe<sub>2</sub>

Sulfur dioxide (0.858 g) and C<sub>2</sub>H<sub>4</sub> (0.125 mmol) were successively added to SNSAsF<sub>6</sub> (0.192 mmol) in a thick-walled 5 mm NMR tube as described above. The mixture was quickly warmed to room temperature and a <sup>1</sup>H NMR spectrum was recorded, showing formation of a mixture of cations **1a** and **2a** (Fig. 1). Similar experiments were performed for the reactions of *cis*-MeHCCHMe (0.0570 mmol) and H<sub>2</sub>CCMe<sub>2</sub> (0.0985 mmol) with SNSAsF<sub>6</sub> (0.0958 and 0.118 mmol respectively) in SO<sub>2</sub> (0.878 and 0.854 g respectively). Proton NMR spectra showed that both reactions of *cis*-MeHCCHMe and H<sub>2</sub>CCMe<sub>2</sub> gave a mixture of cations **1** and **2** and their spectral data are given in Fig. 1. The intensities remained unchanged over time. The ratios *k*<sub>2</sub>/*k*<sub>1</sub> for C<sub>2</sub>H<sub>4</sub>, *cis*-MeHCCHMe and H<sub>2</sub>CCMe<sub>2</sub> were estimated using equation (7) (see below) in which the concentrations of the cycloadducts were determined from NMR integrations. Actual spectra have been deposited.

#### Theoretical calculations on cations **1a** and **2a**

The structures of cations **1a** and **2a** were optimized at the restricted Hartree-Fock (RHF)/6-31G\* level with the GAUSSIAN 92/DFT suite of programs,<sup>12a</sup> using experimental (**2a**, see Table 6)<sup>6</sup> and estimated geometries (**1a**: S–N 1.65, S–C 1.81 and C–C 1.51 Å; S–N–S 112, N–S–C 102 and S–C–C 112°). The optimized geometry for **1a** (C<sub>1</sub> symmetry, see Table 7) results in a slight puckering of the five-membered ring (dihedral angles C–C–S–N -19.32, C–S–N–S 6.40°), presumably caused by staggering of the CH<sub>2</sub> groups, as illustrated by the structure in Table 7. The stationary-point structure is in a very shallow potential-energy well; the planar five-membered ring with

**Table 1** Data for the reactions of SNSAsF<sub>6</sub> with alkenes in liquid SO<sub>2</sub>

Amount of reagent/g (mmol)			Recovered product			Analyses (%) <sup>c</sup>				Proposed product
SNSAsF <sub>6</sub>	Alkene	SO <sub>2</sub>	g (mmol)	Yield <sup>a</sup> (%)	D.p. <sup>b</sup> (°C)	S	N	C	H	
0.532 (1.99)	C <sub>2</sub> H <sub>4</sub>	4.70	0.525 (1.78)	89	186	21.7 (21.7)	4.9 (4.8)	8.1 (8.1)	1.3 (1.4)	(S <sub>2</sub> NC <sub>2</sub> H <sub>4</sub> )AsF <sub>6</sub> <b>1a</b>
0.230 (0.87)	<i>trans</i> -MeHCCHMe	3.19	0.260 (0.82)	94	178	19.8 (19.8)	4.3 (4.4)	14.8 (14.9)	2.3 (2.5)	[S <sub>2</sub> N( <i>trans</i> -MeHCCHMe)]AsF <sub>6</sub> <b>1b</b>
0.590 (2.20)	C <sub>7</sub> H <sub>10</sub>	7.94	0.723 (2.10)	95	162	17.9 (17.8)	4.1 (3.9)	22.3 (23.3)	2.7 (2.8)	(S <sub>2</sub> NC <sub>7</sub> H <sub>10</sub> )AsF <sub>6</sub> <b>1g</b>
0.560 (2.08)	C <sub>2</sub> H <sub>4</sub>	2.81	0.670 (2.08)	100	188	20.4 (19.9)	4.5 (4.3)	15.2 (14.9)	2.4 (2.5)	[S <sub>2</sub> N(C <sub>2</sub> H <sub>4</sub> ) <sub>2</sub> ]AsF <sub>6</sub> <sup>d</sup> <b>2a</b>
0.534 (2.00)	<i>trans</i> -MeHCCHMe	3.64	0.674 (1.78)	89	114	17.0 (16.9)	3.6 (3.7)	25.7 (25.3)	4.3 (4.3)	[S <sub>2</sub> N( <i>trans</i> -MeHCCHMe) <sub>2</sub> ]AsF <sub>6</sub> <b>2b</b>
0.170 (0.64)	C <sub>7</sub> H <sub>10</sub>	5.97	0.250 (0.56)	93	206	14.1 (14.1)	3.1 (3.1)	36.7 (36.9)	4.3 (4.4)	[S <sub>2</sub> N(C <sub>7</sub> H <sub>10</sub> ) <sub>2</sub> ]AsF <sub>6</sub> <sup>e</sup> <b>2g</b>
0.353 (1.32)	H <sub>2</sub> CCHMe	5.37	0.490 (1.40)	106 <sup>f</sup>						Mixture of several isomers of [S <sub>2</sub> N(H <sub>2</sub> CCHMe) <sub>2</sub> ]AsF <sub>6</sub> <sup>g</sup>

<sup>a</sup> The yield of isolated product was calculated from the limiting reagent. <sup>b</sup> Decomposition point. <sup>c</sup> Calculated values in parentheses. <sup>d</sup> Identified by full crystal structure determination. <sup>e</sup> Crystallographic data: *M* = 361, monoclinic, *a* = 11.84, *c* = 6.63 Å, β = 101.80°, *U* = 612.82 Å<sup>3</sup>. The crystal was fragile and shattered before a full determination could be completed, and subsequent attempts to obtain suitable crystals were unsuccessful. <sup>f</sup> The reaction of SNSAsF<sub>6</sub> and H<sub>2</sub>CCHMe produced a soluble brown tar; the yield given for this reaction was determined by the net mass increase observed for the vessel and its contents. <sup>g</sup> Infrared and <sup>1</sup>H NMR spectra of the soluble brown tar were complex. IR (neat film, KBr plates):  $\tilde{\nu}_{\max}/\text{cm}^{-1}$  3080m, 3020ms, 2970ms, 2940m, 2875w, 1460ms, 1453ms, 1435ms, 1385ms, 1305w, 1270w, 1230m, 1163w, 1090w, 1050w, 1005m, 910w, 848m, 815s, 792m, 770s, 696vs, 601m, 575ms, 527m, 505ms, 458m and 396s.

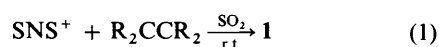
eclipsed CH<sub>2</sub> groups (imposed C<sub>2v</sub> symmetry for geometry optimization) gave an optimized structure 1.6 kJ mol<sup>-1</sup> higher in energy than that of the stationary-point structure. The optimized geometry parameters for **2a** (C<sub>2v</sub> symmetry) are given in Table 6, and are in excellent agreement with the experimental crystal structure data,<sup>6</sup> giving confidence that the calculated structure for **1a** is reasonable.

Vibrational frequencies for cations **1a** and **2a** were calculated at the RHF/6-31G\* level from the optimized geometries. All 21 expected vibrations for **1a** (39 for **2a**) are both Raman- and IR-active for C<sub>1</sub>, C<sub>2</sub> or C<sub>2v</sub> symmetries. Frequencies were scaled by the usual correction factor of 0.89.<sup>12b</sup> Calculated frequencies for the S–N vibrations are listed with the experimental frequencies in Table 3; a complete listing of calculated frequencies for **1a** and **2a** has been deposited. The calculated frequencies are in general agreement with the observed, especially for **2a**. Experimental IR and FT-Raman spectra for **1a** are shown in Fig. 4, and the experimental and calculated Raman frequencies are listed as a footnote in Table 3. All other IR spectra have been deposited.

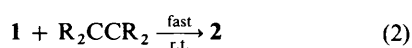
## Results and Discussion

### Preparation and identification of the AsF<sub>6</sub><sup>-</sup> salts of cations **1** and **2**

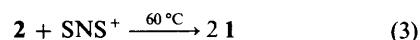
The reactions of SNS<sup>+</sup> (as the AsF<sub>6</sub><sup>-</sup> salt) with alkenes [C<sub>2</sub>H<sub>4</sub>, *trans*- and *cis*-MeHCCHMe, H<sub>2</sub>CCMe<sub>2</sub>, MeHCCH<sub>2</sub> and norbornene (C<sub>7</sub>H<sub>10</sub>)] in 1:1 molar ratios in liquid SO<sub>2</sub> at room temperature (r.t.) led to mixtures of the AsF<sub>6</sub><sup>-</sup> salts of cations **1** and **2**. Therefore under these conditions, the 1:1 cycloadducts **1** formed from the first cycloadditions of SNS<sup>+</sup> with alkenes [equation (1)] underwent a second cycloaddition with another



of the alkene molecules to give **2** [equation (2)] and the second cycloadditions were apparently faster than the first.



The 1:1 cycloadducts **1a**, **1b** and **1g** were quantitatively prepared by the reactions of SNSAsF<sub>6</sub> with the respective alkene H<sub>2</sub>CCH<sub>2</sub>, *trans*-MeHCCHMe and C<sub>7</sub>H<sub>10</sub> in the molar ratio 1:1 in liquid SO<sub>2</sub> at 60–70 °C (Table 1). Their purity was established by chemical analyses (Table 1) and IR (Table 2) and multinuclear NMR spectroscopy (<sup>1</sup>H, <sup>13</sup>C, <sup>14</sup>N) (Figs. 1 and 2). At this temperature the 1:2 cycloadduct **2** (formed from the second cycloaddition reaction) likely undergoes a thermal dissociation to **1** and free alkene [the reverse of the second cycloaddition in equation (2)]. The liberated alkene then reacts with unreacted SNSAsF<sub>6</sub> to give **1** [equation (1)]. The thermal dissociation of the 1:2 cycloadduct **2** was demonstrated from the reactions of SNSAsF<sub>6</sub> with the AsF<sub>6</sub><sup>-</sup> salts of **2a** and **2g** in the molar ratio 1:1 at 60–70 °C (Table 5), leading to a quantitative formation of pure **1** [equation (3)]. For



Me<sub>2</sub>CCMe<sub>2</sub>, the second cycloaddition did not take place, probably because of steric effects (discussed below). Therefore, we were not able to prepare **2e** by the reaction of SNSAsF<sub>6</sub> even with a large excess of Me<sub>2</sub>CCMe<sub>2</sub> at room temperature.

The 1:2 cycloadducts **2a**, **2b** and **2g** were prepared quantitatively by the reactions of SNSAsF<sub>6</sub> with the corresponding alkenes in the molar ratio 1:2 in liquid SO<sub>2</sub> at room temperature (Table 1). Their purity was also established by chemical analyses (Table 1) and IR (Table 2) and multinuclear NMR spectroscopy (<sup>1</sup>H, <sup>13</sup>C, <sup>14</sup>N) (Figs. 1 and 2). In addition, they were also prepared in essentially quantitative yield by the cycloaddition reactions of **1** with the corresponding alkenes. The mixed-alkene cation **2f** was also prepared from the cycloaddition reactions of **1a** with *trans*-MeHCCHMe or **1b** with C<sub>2</sub>H<sub>4</sub>, characterized *in situ* by <sup>1</sup>H and <sup>13</sup>C NMR (Table 4, Fig. 1). Prior to our preliminary account, derivatives of both **1** and **2** had not been reported. Since then, **2g** has been obtained by the reaction of norbornene with S<sub>3</sub>N<sub>3</sub>Cl<sub>3</sub> followed by thermolysis of the adduct.<sup>11</sup> A partially characterized compound described as neutral 2-methyl-1,3,2-dithiazolidine<sup>10</sup> had been prepared in low yield (ca. 5%) from the reaction of methylamine and ethane-1,2-disulphenyl

**Table 2** Infrared spectral data (cm<sup>-1</sup>) of [S<sub>2</sub>N(alkene)]AsF<sub>6</sub> **1** and [S<sub>2</sub>N(alkene)]AsF<sub>6</sub> **2**

[S <sub>2</sub> NC <sub>2</sub> H <sub>4</sub> ]AsF <sub>6</sub> <b>1a</b>	[S <sub>2</sub> N(C <sub>2</sub> H <sub>4</sub> ) <sub>2</sub> ]AsF <sub>6</sub> <b>2a</b>	[S <sub>2</sub> N( <i>trans</i> - MeHCCHMe)]AsF <sub>6</sub> <b>1b</b>	[S <sub>2</sub> N( <i>trans</i> - MeHCCHMe <sub>2</sub> )]AsF <sub>6</sub> <b>2b</b>	(S <sub>2</sub> NC <sub>7</sub> H <sub>10</sub> )AsF <sub>6</sub> <b>1g</b>	[S <sub>2</sub> N(C <sub>7</sub> H <sub>10</sub> ) <sub>2</sub> ]AsF <sub>6</sub> <b>2g</b>	Tentative assignments <sup>b</sup>
3015m 2950m	3042ms 2980ms	2960m 2920 (sh) 2860w	2962s 2918s 2865m	2945ms 2870m	2960s 2870s	v(C-H) stretch v(CH <sub>2</sub> )(CH <sub>3</sub> ) C-H stretch
1426m 1412ms	1582m 1552m 1425ms	1450m	1448s 1438 (sh) 1388m 1379ms 1373m	1456m	1457m 1427s	CH <sub>3</sub> def.
1338m	1380m 1313s	1380m 1313s	1373m	1313m 1300ms	1325m 1312m 1302w 1265w	v(C-C) stretch
1240m	1253m	1275s	1251m	1256m 1236ms 1206m 1190m	1250w 1228w 1207m	Ring vibrations
1087vw	1081w 1032s	1079m 1045m 1025w 1006m	1117w	1076w 1019w	1179m 1168m 1127w 1105w	Ring vibrations
987s	989m 977m 967m	985 (sh) 963s	991s 977m	993s 956w 940w 923w	997w 946m 925w	CH <sub>3</sub> , CH <sub>2</sub> rock
920vw	894w 819ms	912w 898w 850w		886w 863w		C-C stretch and ring vibrations
791s	778ms 698vs	788m 700vs	795s 752s 690vs	789s 767w 700vs	869m 829w 805m 775w 696vs 675 (sh)	v <sub>asym</sub> (SN) v <sub>sym</sub> (SN) v <sub>3</sub> (AsF <sub>6</sub> )
630 (sh)	616m 576w	583m 552m	600w 572m	616s 572w 547m	542s 510w	C-S stretch and v <sub>2</sub> (AsF <sub>6</sub> <sup>-</sup> )
579vw 552m 529w 498w	465ms	483 (sh)	528m 493s			δ(SNS)
397s	396s	393s	449s 388s	397s	452m 398s	v <sub>4</sub> (AsF <sub>6</sub> <sup>-</sup> )

<sup>a</sup> Spectra have been deposited. <sup>b</sup> Supported by calculated (RHF/6-31G\*) frequencies (deposited).

**Table 3** Observed and theoretical (RHF/6-31G\*) SN vibrational wavenumbers (cm<sup>-1</sup>) for S<sub>2</sub>NC<sub>2</sub>H<sub>4</sub><sup>+</sup> **1a** and S<sub>2</sub>N(C<sub>2</sub>H<sub>4</sub>)<sub>2</sub><sup>+</sup> **2a**. Full tables have been deposited. Experimental spectra for **1a** are shown in Fig. 4

SNS(C <sub>2</sub> H <sub>4</sub> ) <sup>+</sup> <b>1a</b>			SNS(C <sub>2</sub> H <sub>4</sub> ) <sub>2</sub> <sup>+</sup> <b>2a</b>		
IR	FT-Raman <sup>a</sup>	Calculated <sup>b</sup> (IR, Raman relative intensity)	IR	Calculated <sup>b</sup> (IR, Raman relative intensity)	Assignment <sup>c</sup>
893vs		862 (100, 1)	819ms	818 (100, 0)	v <sub>asym</sub> (SNS)
791s	788(100)	783 (5, 3)	under AsF <sub>6</sub> <sup>-</sup> ?	730 (65, 5)	v <sub>sym</sub> (SNS)
529w	547(40)	526 (1, 3)	616m <sup>d</sup>	612 (0, 14)	δ(SNS)

<sup>a</sup> Experimental FT-Raman spectrum:  $\tilde{\nu}_{\max}/\text{cm}^{-1}$ (relative intensity) 153(40), 218(45), 369(20) [v<sub>4</sub>(AsF<sub>6</sub><sup>-</sup>)], 472(30), 547(40), 628(25), 680(45) [v<sub>3</sub>(AsF<sub>6</sub><sup>-</sup>)], 788(100), 2963(55). Calculated Raman spectrum:  $\tilde{\nu}_{\max}/\text{cm}^{-1}$  124(0.4) (ring def.), 351(0.3) (ring def.), 483(7.3) [v(CS)], 526(2.7) [δ(SNS) in plane], 622(15.9) [v(CS)], 648(1.9) [v(CS)], 783(3.0) [v<sub>sym</sub>(SN)], 798(0.7) [τ(CC) in plane], 862(1.1) [v<sub>asym</sub>(SN)], 950(3.0) [v(CC)], 962(0.6) [v(CC)], 1094(0.3) [v(CH<sub>2</sub>)], 1172(3.2) [v(CH<sub>2</sub>)], 1278(2.9) [v(CH<sub>2</sub>)], 1292(0.4) [v(CH<sub>2</sub>)], 1426(9.6) [v(CH<sub>2</sub>)], 1447(5.9) [v(CH<sub>2</sub>)], 2910(33.2) [v(CH<sub>2</sub>)], 2914(100.0) [v(CH<sub>2</sub>)], 2968(42.3) [v(CH<sub>2</sub>)] and 2980(46.8) [v(CH<sub>2</sub>)]. <sup>b</sup> Due to extensive mixing, as expected for ring compounds incorporating heavy atoms (e.g. SNSNS<sup>2+</sup>),<sup>12i</sup> almost all calculated frequencies showed some contribution from S–N bonds. The values listed were those for which the S–N bonds were the most significant contributions to the vibration. Full listings of the theoretical vibrational analysis from GAUSSIAN 92 have been deposited. <sup>c</sup> An estimate of the expected S–N stretch (average of v<sub>sym</sub> and v<sub>asym</sub>) may be made from the observed S–N bond length using Banister's<sup>12b</sup> correlation:  $\lambda(\text{S-N}) = 0.1941d(\text{S-N}) - 20.66$  where  $d(\text{S-N})$  is the bond length in pm and  $\lambda(\text{SN})$  is 10<sup>4</sup> times the reciprocal of the corresponding wavenumber value of  $\nu$ . For **1a**, the calculated S–N bond distance of 1.575 Å corresponds to a calculated wavenumber of 1009 cm<sup>-1</sup>. For **2a**, the observed distance 1.634 Å corresponds to 905 cm<sup>-1</sup>. Note that the data for this correlation were compiled from SN- and S<sub>2</sub>N-containing compounds, not S<sub>2</sub>N-containing compounds. However, this does support the assignment of 783 cm<sup>-1</sup> for **1a** being higher than 730 cm<sup>-1</sup> for **2a**. <sup>d</sup> Note that from the theoretical calculations this mode is IR inactive.

**Table 4** Reactions of [S<sub>2</sub>N(alkene)]AsF<sub>6</sub> **1** with alkenes and acetylene in liquid SO<sub>2</sub>

Amount of reagent/g (mmol)					
[S <sub>2</sub> N(alkene)]AsF <sub>6</sub>	Substrate	SO <sub>2</sub>	Observations and conditions <sup>a</sup>	Product(s) <sup>b</sup>	
(S <sub>2</sub> NC <sub>2</sub> H <sub>4</sub> )AsF <sub>6</sub>	C <sub>2</sub> H <sub>4</sub>	0.70	Clear yellow to colourless	S <sub>2</sub> N(C <sub>2</sub> H <sub>4</sub> ) <sub>2</sub> <sup>+</sup> <b>2a</b> (0.20 mmol)	
0.057 (0.19)	0.007 (0.25)				
0.035 (0.12)	<i>trans</i> -MeHCCHMe	0.70	Clear yellow to colourless	<i>trans</i> -MeHCCHMe (0.06 mmol), S <sub>2</sub> N(C <sub>2</sub> H <sub>4</sub> )( <i>trans</i> -MeHCCHMe) <sup>+</sup> <b>2f</b> (0.10 mmol) <sup>c</sup>	
	0.009 (0.16)				
0.029 (0.10)	C <sub>2</sub> H <sub>2</sub> <sup>d</sup>	0.70	Clear yellow to colourless	C <sub>2</sub> H <sub>2</sub> (0.15 mmol), HCSNSCH <sup>+</sup> (0.05 mmol), <b>2a</b> (0.06 mmol) <sup>e</sup>	
	0.006 (0.26)				
[S <sub>2</sub> N( <i>trans</i> -MeHCCHMe)]AsF <sub>6</sub>	<i>trans</i> -MeHCCHMe	4.87	Clear yellow to red to colourless <sup>f</sup>	[S <sub>2</sub> N( <i>trans</i> -MeHCCHMe) <sub>2</sub> ] <sup>+</sup> AsF <sub>6</sub> <b>2b</b> (0.35 g, 0.92 mmol, 90% yield) <sup>g</sup>	
0.33 (1.03)	0.47 (8.33)	0.78	Clear yellow to red to colourless	C <sub>2</sub> H <sub>4</sub> (0.17 mmol), <b>2b</b> (0.01 mmol), <b>2f</b> (0.05 mmol) <sup>c</sup>	
0.032 (0.10)	C <sub>2</sub> H <sub>4</sub>				
	0.008 (0.28)				
0.035 (0.11)	C <sub>2</sub> H <sub>2</sub> <sup>d</sup>	0.63	Clear yellow to red to colourless	C <sub>2</sub> H <sub>2</sub> (0.18 mmol), HCSNSCH <sup>+</sup> (0.05 mmol), <b>2b</b> (0.05 mmol), <i>trans</i> -MeHCCHMe (0.03 mmol)	
	0.007 (0.26)				

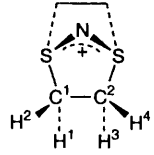
<sup>a</sup> 5 min after addition of reagents to end of reaction time period at room temperature for 1 h unless specified. <sup>b</sup> Unless specified otherwise the products were identified *in situ* by <sup>1</sup>H NMR spectroscopy, by comparison of the observed spectrum with the data given in Fig. 1 and in ref. 2(a) (for HCSNSCH<sup>+</sup>). The yields of these reactions were calculated from the integration of the assigned resonances with respect to an internal concentration standard, CH<sub>2</sub>Cl<sub>2</sub> (typically 0.10–0.30 mmol). The estimated error in these measurements is approximately ±15%. <sup>c</sup> Proton NMR data in Fig. 1, actual spectrum has been deposited. <sup>d</sup> Similar treatment with MeCN led to no reaction. <sup>e</sup> On heating for 2 d at 75 °C HCCH (0.09 mmol), H<sub>2</sub>CCH<sub>2</sub> (0.07 mmol) and HCSNSCH<sup>+</sup> (0.09 mmol) were obtained. <sup>f</sup> Room temperature and 2 h. <sup>g</sup> Recovered yield, the reaction was carried out in a two-bulb vessel. The product was identified by comparison of the IR and NMR spectra with the data given in Table 2 and Fig. 1 respectively.

**Table 5** Data for reactions of [S<sub>2</sub>N(alkene)<sub>2</sub>]<sup>+</sup>AsF<sub>6</sub> **2** with SNSAsF<sub>6</sub> and acetylene in liquid SO<sub>2</sub>

Amount of reagent/g (mmol)					
[S <sub>2</sub> N(alkene) <sub>2</sub> ] <sup>+</sup> AsF <sub>6</sub>	Substrate	SO <sub>2</sub>	Conditions	Observations <sup>a</sup>	Products <sup>b</sup>
[S <sub>2</sub> N(C <sub>2</sub> H <sub>4</sub> ) <sub>2</sub> ] <sup>+</sup> AsF <sub>6</sub>	SNSAsF <sub>6</sub> 0.267 (1.00)	5.76	60 °C, 1 d	Clear yellow to clear yellow	S <sub>2</sub> NC <sub>2</sub> H <sub>4</sub> <sup>+</sup> <b>1a</b> (0.573 g, 1.94 mmol, 100% yield) <sup>c</sup>
0.314 (0.97)					
[S <sub>2</sub> N(C <sub>7</sub> H <sub>10</sub> ) <sub>2</sub> ] <sup>+</sup> AsF <sub>6</sub>	SNSAsF <sub>6</sub> 0.026 (0.10)	0.60	60 °C, 1 d	Colourless to clear yellow	S <sub>2</sub> NC <sub>7</sub> H <sub>10</sub> <sup>+</sup> <b>1g</b>
0.029 (0.06)					
[S <sub>2</sub> N(C <sub>2</sub> H <sub>4</sub> ) <sub>2</sub> ] <sup>+</sup> AsF <sub>6</sub>	C <sub>2</sub> H <sub>2</sub> 0.007 (0.28)	0.59	60 °C, 2 h	Clear yellow to colourless	C <sub>2</sub> H <sub>2</sub> (0.15 mmol), S <sub>2</sub> N(C <sub>2</sub> H <sub>4</sub> ) <sub>2</sub> <sup>+</sup> <b>2a</b> (0.18 mmol), C <sub>2</sub> H <sub>4</sub> (0.05 mmol), HCSNSCH <sup>+</sup> (0.05 mmol)
0.081 (0.25)					
			60 °C, 4 d	Clear yellow to colourless	C <sub>2</sub> H <sub>2</sub> (0.08 mmol), <b>2a</b> (0.05 mmol), C <sub>2</sub> H <sub>4</sub> (0.10 mmol), HCSNSCH <sup>+</sup> (0.15 mmol)

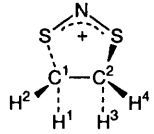
<sup>a</sup> See footnote a in Table 4. <sup>b</sup> See footnote b in Table 4. <sup>c</sup> See footnote g in Table 4.

**Table 6** Comparison of experimental<sup>6</sup> and calculated geometries for  $S_2N(C_2H_4)_2^+$  **2a**. Bond lengths in Å, angles in °; estimated standard deviations (e.s.d.s) refer to the last digit



	Experimental	RHF/6-31G*
$d(S-N)$	1.634(4)	1.633
$d(S-C^1)$	1.814(7)	1.832
$d(S'-C^2)$	1.804(7)	1.832
$d(C^1-C^2)$	1.511(9)	1.541
$d(C^1-H^1)$	0.99(7)	1.080
$d(C^1-H^2)$	1.01(8)	1.081
$d(C^2-H^3)$	0.88(7)	1.080
$d(C^2-H^4)$	1.04(7)	1.081
$S-N-S'$	102.4(4)	103.85
$C-S-N$	99.0(3)	98.58
$C^1-C^2-S'$	107.1(5)	108.13
$C^1-S-C^2$	96.1(3)	96.83

**Table 7** RHF/6-31G\* optimized geometry of  $S_2NC_2H_4^+$  **1a**. Distances in Å, angles in °. Dihedral angles in italics are those responsible for ring puckering



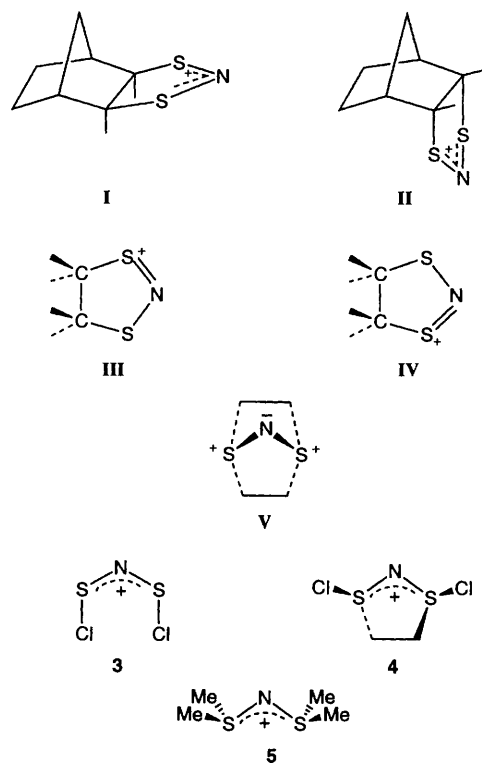
Parameter	Stationary-point ( $C_1$ ) value
$d(C^1-C^2)$	1.529
$d(C-S)$	1.834
$d(S-N)$	1.575
$d(C^1-H^1), (C^2-H^4)$	1.081
$d(C^2-H^2), (C^1-H^3)$	1.082
$C-C-S$	108.02
$C-S-N$	97.96
$S-N-S$	122.61
$C^2-C^1-H^1, C^1-C^2-H^4$	111.58
$C^2-C^1-H^2, C^1-C^2-H^3$	112.45
$C-C-S-N$	-19.32
$C-S-N-S$	6.40
$S-C^2-C^1-H^1, S-C^1-C^2-H^4$	143.51
$S-C^2-C^1-H^2, S-C^1-C^2-H^3$	-93.43

chloride. The preparation of **1** and **2** from the above reactions therefore provides an apparently general route to the two new ring families.

Cations **1a** and **1b** underwent quantitative reactions with  $C_2H_2$  according to equation (4) (alkene =  $C_2H_4$  or *trans*-



MeHCCHMe) to give  $\overline{HCSNSCH}^+$  and **2**, which were identified by  $^1H$  NMR spectroscopy (Table 4). We previously showed that **1a** underwent similar reaction with PhCCPh to give  $\overline{PhCSNSCPh}^+$  and **2a**.<sup>2e</sup> The results are consistent with the expectation that the lower energy of the completely delocalized  $6\pi$   $\overline{HCSNSCH}^+$  (relative to that of the partially delocalized  $4\pi$  **1**) renders reaction (4) thermodynamically favourable (discussed below). Cations **1a** and **1b** did not react with MeCN [ionization potential (MeCN) = 12.2, ( $C_2H_2$ ) = 10.5 eV] likely due to a higher kinetic barrier (see below), although the reaction is thermodynamically favourable.



### Structures of cations **1**

The  $^1H$  and  $^{13}C$  NMR spectra of cations **1** are consistent with planar ring structures (see Figs. 1 and 2) or very rapid equilibrium between the two puckered structures (see below). Resonances attributable to **1** are at higher field than those of the corresponding alkene, consistent with higher shielding in the alkane and the effect of the positive charge. The  $^1H$  spectrum of **1a** has a singlet at  $-70$  °C with a linewidth similar to that at room temperature showing equivalence of the protons on the NMR time-scale down to  $-70$  °C. The  $^{14}N$  NMR chemical shifts of **1** lie in a narrow range ( $120 \leq \delta \leq 148$ ) with large linewidths. The  $^{13}C$  NMR chemical shift range ( $22 \leq \delta \leq 82$ ) is also narrow as predicted by Mason.<sup>13b</sup> Thus a combination of  $^{13}C$  and  $^{14}N$  chemical shifts is likely to be diagnostic for derivatives of this family of heterocycles.

Two isomers are possible for cation **1g**, *exo* **I** or *endo* **II**. The former configuration is expected as all sulfur-nitrogen adducts of norbornadiene (bicyclo[2.2.1]hepta-2,5-diene) so far observed adopt *exo* structures.<sup>13c</sup> The *exo* structure is assigned by comparison of the observed  $^1H$  and  $^{13}C$  NMR spectra with those of the related  $S_3C_7H_{10}$ <sup>13d</sup> (*exo* from X-ray structure<sup>13e</sup>) and **2g** (Fig. 2). Of particular note are the similarities of the  $^4J(H_a, H_c)$  couplings for all three,  $S_3C_7H_{10}$ <sup>13d</sup> (2.1), **1g** (1.8) and **2g** (1.5 Hz), indicative of *exo* configurations and arising from 'W coupling'.<sup>13f</sup> It is likely that cycloaddition of norbornadiene to  $SNS^+$  is less hindered sterically from the bridgehead side.

### Calculated geometry and electronic structure of cation **1a**

Since no crystal structure of cations **1** was obtained, the structure of **1a** was calculated by *ab initio* methods (see Table 7). Confidence in the results at the RHF/6-31G\* level is supported by the good agreement between the calculated and experimentally observed<sup>6</sup> geometries of the related **2a** (Table 6) and a comparison of the calculated geometry of **1a** and the experimental geometries of related species, shown in Table 8. The calculated S-N distance in **1a** (1.575 Å) is slightly longer than that found in  $CISNSCl^+$  **3** (1.528 Å)<sup>12c</sup> containing more electronegative substituents, as observed in  $RSN$ ,  $R_2SO$ ,  $R_2SO_2$  and related compounds.<sup>13a</sup> The calculated charges on sulfur (0.70) and nitrogen (-0.42) and the S-N bond order

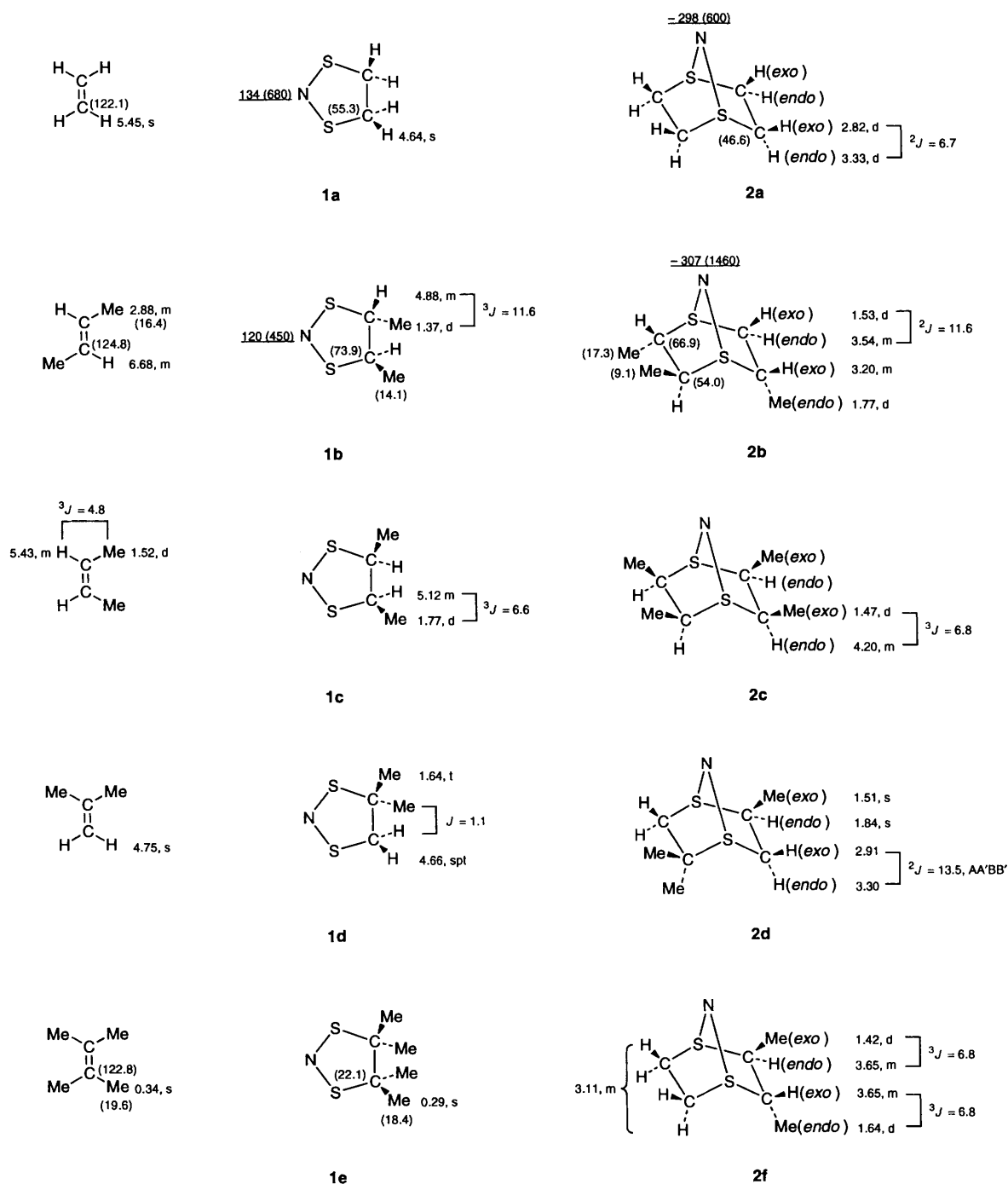


**Fig. 1** Multinuclear NMR spectral data (chemical shifts in  $\delta$ , coupling constants in Hz) for the alkenes ( $C_2H_4$ , *trans*- and *cis*- $MeHCCHMe$ ,  $Me_2CCH_2$  and  $Me_2CCMe_2$ ), cations **1** and **2** given as  $^1H$  with  $^{13}C$  in parentheses and  $^{14}N$  underlined (width at half height in Hz in parentheses). s = Singlet, d = doublet, t = triplet, spt = septet and m = multiplet. The spectrum of **1b** was analysed as an  $AA'X_3X'_3$  pattern using a modified version of the LAOCN 5 simulation program,<sup>9</sup> giving good agreement between the observed and calculated [ $J_{AA'} = 2.42$ ,  $J_{AX} = J_{A'X'} = 7.38$ ,  $J_{AX'} = J_{A'X} = -0.17$  ( $J_{AA'}$  and  $J_{AX}$  assumed positive),  $J_{XX'} = 0.00$  Hz] spectra. The spectra have been deposited

(1.7) indicate that **1a** may be represented by valence-bond structures **III** and **IV** with some polarization of charge onto nitrogen and increase in positive charge on sulfur.

Cation **2a** may be represented by structure **V** with lesser contributions from S=N-containing structures formed by transfer of negative charge from  $N^-$  to  $S^+$ . Consequently the  $^{14}N$  NMR chemical shifts indicate the nitrogen atom of **1a** ( $\delta$  134) is shielded less than that of **2a** ( $\delta$  -298) which has a larger negative charge on nitrogen (calc., -0.83; valence-bond structure **V**, -1.0).

The calculated geometry of cation **1a** is puckered with an S-C-C-S dihedral angle of  $24.2^\circ$  similar to that found ( $27.4^\circ$ ) experimentally for **4**<sup>13a</sup> (see Table 8). In contrast to **1a**, the  $^1H$  NMR spectrum of **4**<sup>13a</sup> shows an  $AA'BB'$  pattern as expected as

the cation contains a puckered ring and staggered  $CH_2$  groups. The solid-state structure of the related **3** is planar,<sup>12c</sup> and although the observed geometry is reasonable due to  $\pi$  back bonding from the halogen atoms this back bonding is not possible in derivatives of **2** which therefore adopt non-planar structures. The planar structure of **1a** is calculated to be only  $1.6 \text{ kJ mol}^{-1}$  higher in energy than the puckered ground state. The two equivalent puckered forms of **1a** are probably in rapid equilibrium with a very low (less than  $2 \text{ kJ mol}^{-1}$ ) energy barrier, rendering the protons equivalent on the NMR time-scale. Reasonably, other more bulky derivatives of **1** would be more strained in the planar form and favour the puckered configuration. However the room-temperature  $^1H$  NMR spectra of the other symmetrical derivatives of **1** suggest that

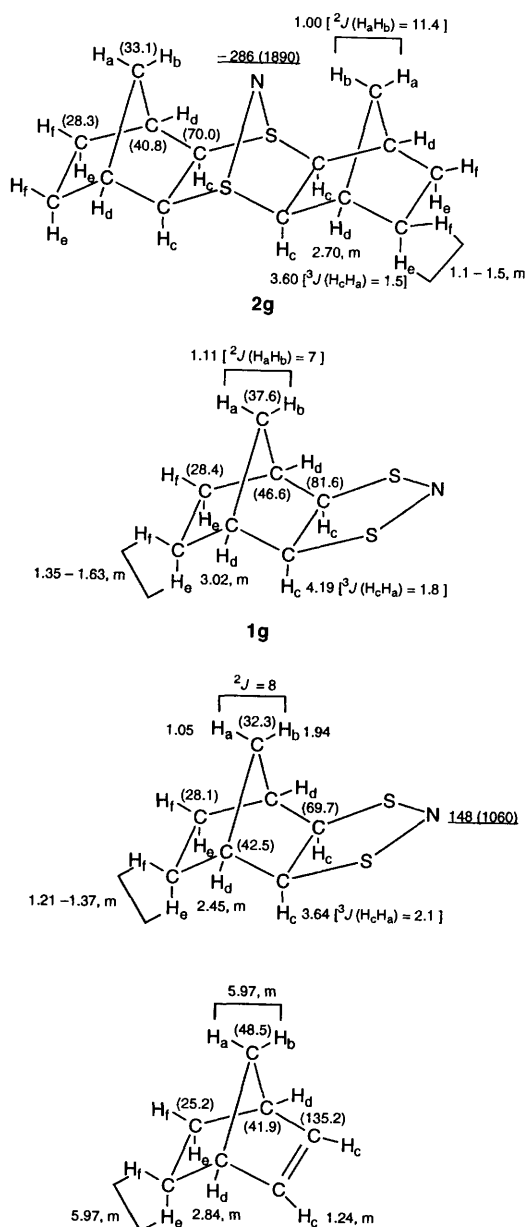


**Fig. 2** Comparison of the multinuclear NMR<sup>a</sup> data for C<sub>7</sub>H<sub>10</sub> (this work), S<sub>3</sub>C<sub>7</sub>H<sub>10</sub>,<sup>10</sup> **1g** and **2g** presented as in Fig. 1. The spectra have been deposited. The difference (1.2 ppm) between the <sup>13</sup>C chemical shifts reported<sup>11</sup> for **2g** prepared from S<sub>3</sub>N<sub>3</sub>Cl<sub>3</sub> and norbornene ( $\delta$  29.5, 34.3, 42.0 and 71.3) with those of **2g** arises as our reference is SiMe<sub>4</sub> in SO<sub>2</sub>, however Chivers and co-workers used SiMe<sub>4</sub> in CDCl<sub>3</sub>. On selectively decoupling H<sub>c</sub> in **1g** and **2g** the doublet of heptets assigned to H<sub>a</sub> simplified to a doublet of quartets. The <sup>14</sup>N NMR spectra were acquired at 360 MHz by the Atlantic NMR Centre at Dalhousie University

the rings are planar or, more likely in view of the above, that there is rapid equilibrium between two puckered structures with a low energy barrier to interconversion.

#### Structures of cations **2** and steric effects on cycloaddition of alkene to **1**

The similarity of the <sup>13</sup>C (28 ≤  $\delta$  ≤ 67) and <sup>14</sup>N (−307 ≤  $\delta$  ≤ −286) chemical shifts of cations **2a**, **2b** and **2g** for ring carbon and nitrogen atoms strongly implies that they all have the same norbornene-like structure as that of **2a**, the crystal structure of which has been determined,<sup>6</sup> and that these chemical shift ranges are diagnostic for this ring system. The structures of **2c**, **2d** and **2f**, and the conformations of **2a**, **2b** and **2g**, were determined from their <sup>1</sup>H NMR spectra (see Figs. 1 and 2) and further supported by the <sup>13</sup>C NMR spectra of

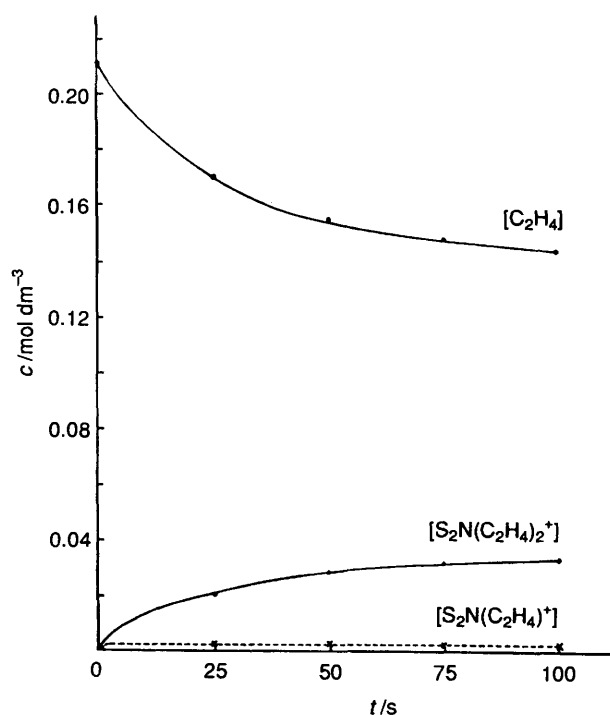
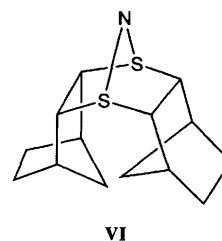


**Fig. 3** Change of concentration of C<sub>2</sub>H<sub>4</sub>, **1a** and **2a** with time for the reaction of SNSAsF<sub>6</sub> and C<sub>2</sub>H<sub>4</sub> in liquid SO<sub>2</sub> at room temperature



the substituent groups for **2a**, **2b** and **2g**. Only one isomer was observed for **2b–2d** and **2g** whereas two or more are possible in each case (see Fig. 5), i.e. these cycloadditions are stereospecific. However, a mixture of isomers was observed for S<sub>2</sub>N(MeHCCH<sub>2</sub>)<sub>2</sub><sup>+</sup> [Fig. 5(a)] and we were unable to prepare S<sub>2</sub>N(Me<sub>2</sub>CCMe<sub>2</sub>)<sub>2</sub><sup>+</sup> [Fig. 5(e)]. These facts imply that either the intrinsic thermodynamic instability or the energy of the transition state is highest for products containing adjacent *endo*-methyl/*endo*-methyl [**2d**\* in Fig. 5(c)], and lowest in energy for two adjacent *endo*-hydrogens [**2c** in Fig. 5(b)]. In between is the case for adjacent *endo*-methyl/*endo*-hydrogen [**2c**\* in Fig. 5(b)]. This suggests that all the *endo*-hydrogen isomers of S<sub>2</sub>N(MeHCCH<sub>2</sub>)<sub>2</sub><sup>+</sup> [x and y in Fig. 5(a)] are likely to be favoured but that the isomer containing adjacent *endo*-methyls [z in Fig. 5(a)] will not be present in the mixture. The steric unfavourability of *endo*-methyl implies that the *exo*- $\beta$ ,*exo*- $\beta$  isomer **VI** of the **2g** type molecule (Fig. 2) can be excluded, and this is supported by severe steric crowding in a space-filling model.

#### FMO analysis of the concerted symmetry-allowed cycloaddition reactions of SNS<sup>+</sup> with alkenes

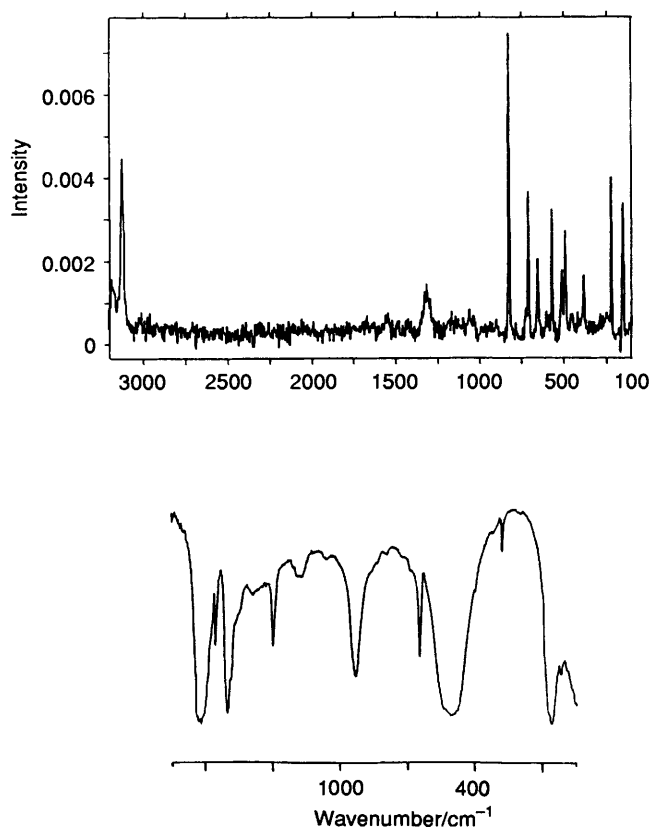
Frontier molecular orbital theory has been successfully employed in the analysis of cycloaddition reactions of SNS<sup>+</sup> with alkynes and nitriles, and we have shown that these cycloadditions are concerted and symmetry allowed, and that they proceed *via* the dominant interactions of the  $\pi^*$  LUMO of SNS<sup>+</sup> with  $\pi$  HOMOs of simple alkynes and nitriles.<sup>2d</sup> The symmetry and relative energies of the frontier orbitals shown in Figs. 6 and 9 imply that alkenes would undergo a similar



**Table 8** Comparison of  $S_2NC_2H_4^+$  **1a** with related compounds

Cation	$d(S-C)/\text{\AA}$ , b.o. <sup>a</sup>	$d(C-C)/\text{\AA}$ , b.o. <sup>a</sup>	$d(S-N)/\text{\AA}$ , b.o. <sup>b</sup>	S-N-S [estimated from $d(S-N)]^\circ$	S-N-S/ $^\circ$	Charge on S, N <sup>d</sup>	<sup>14</sup> N NMR shift, $\delta$	Ref.
<b>3</b> CISNSCI <sup>+</sup>	—	—	1.528, 1.97	151.3	151.0	0.76, -0.46	19	This work, 12(c), 13(a)
<b>1a</b> $S_2NC_2H_4^+$ calc. geom.	1.834, 0.92	1.529, 1.0	1.575, 1.73	130.7	122.6	0.70, -0.42	134	This work, 2(g), 13(a)
<b>4</b> $\overline{CH_2(SCI)N(SCI)CH_2}^+$	1.822, 1.0	1.504, 1.1	1.603, 1.58	118.1	115.3	0.94, -0.80	-243	13(a)
<b>2a</b> $S_2N(C_2H_4)_2^+$ obs. geom.	1.809, 1.0	1.511, 1.1	1.634, 1.41	104.4	102.4	0.89, -0.83	-298	This work, 2(g), 6
calc. geom.	1.832, 0.93	1.541, 1.0	1.633, 1.41	104.7	103.9			
<b>5</b> $Me_2SNSMe_2^+$	1.80, 1.0	—	1.64, 1.38	101.8	110.8	0.91, -0.89		This work 12(d)

<sup>a</sup> Bond order (b.o.) calculated by the equation  $D_n = D_1 - 0.71 \log(\text{b.o.})$ , where  $D_1$  is the length of a formal single bond (S-C 1.81 Å, C-C 1.54 Å).<sup>12f</sup> <sup>b</sup> For S-N bonds in which the N contains a non-bonding lone pair the bond order is related to the bond length  $d(S-N)/\text{\AA}$  by the equation  $\text{b.o.}(S-N) = 0.429 + 6.850d(S-N) - 3.825d(S-N)^2$ .<sup>12g</sup> <sup>c</sup> Banister *et al.*<sup>12e</sup> have shown that for cations containing an SNS unit the S-N bond length (pm) is related to the S-N-S bond angle ( $^\circ$ ) by the equation  $d(S-N) = 187.03 - 0.2263(\text{angle at N})$ . <sup>d</sup> From GAUSSIAN 92/DFT Mulliken population analysis.

**Fig. 4** FT-Raman (top) and IR (bottom, Nujol mull) spectra of cation **1a**

reverse-electron-demand concerted symmetry-allowed cycloaddition reaction.

The cation  $SNS^+$  has two mutually perpendicular (three-centre, four-electron)  $\pi$  manifolds, whereas an alkene molecule has only one (two-centre, two-electron), so that the formation of a purely  $\sigma$ -bonded hydrocarbon moiety upon 1:1 cycloaddition of an alkene to  $SNS^+$  can be viewed from the simple Hückel level as leaving the second  $\pi$  system of the bent SNS fragment on **1** unaffected. This conclusion was further confirmed by STO-3G calculations (Fig. 6). Therefore, a second concerted symmetry-allowed cycloaddition reaction of **1** with an alkene reasonably proceeds *via* the interaction between the  $\pi$  HOMO of the alkene and the  $\pi^*$  LUMO of **1**, the energy difference ( $\Delta E_2$ ) being higher than that between the LUMO of the parent  $SNS^+$  and the HOMO of the alkene ( $\Delta E_1$ ). This implies that the rate of the second cycloaddition would be

slower than the first. However, our preliminary observations implied that this was not the case, which motivated quantitative studies of the reaction kinetics.

#### Kinetic aspects and electronic features of the cycloadditions of $SNS^+$ and cations **1** with alkenes ( $C_2H_4$ , *cis*-MeHCCHMe and $H_2CCMe_2$ )

We have shown above that  $SNS^+$  (as the  $AsF_6^-$  salt) undergoes cycloaddition reactions with alkenes to give **1**, which in turn undergo a second, probably faster, cycloaddition reaction with another alkene molecule to give **2** (with the exception of  $Me_2CCMe_2$ , for which the second cycloaddition does not occur). The rapid and quantitative nature of the cycloaddition reactions of  $SNS^+$  with alkenes is indicative of a concerted, symmetry-allowed process as expected from a simple FMO analysis.

For the two consecutive cycloadditions (1) and (2) the rate equations are (5) and (6) where  $k_1$  and  $k_2$  represent the rate

$$-d[\text{alkene}]/dt = k_1[\text{alkene}][SNS^+] + k_2[\text{alkene}][\mathbf{1}] \quad (5)$$

$$d[\mathbf{1}]/dt = k_1[\text{alkene}][SNS^+] - k_2[\text{alkene}][\mathbf{1}] \quad (6)$$

constants for the 1:1 [equation (1)] and 1:2 [equation (2)] cycloadditions respectively. The earlier observations showed that the second cycloadditions were apparently faster than the first for the alkenes referred to above, indicating a low-level steady state for **1**, *i.e.*  $d[\mathbf{1}]/dt \approx 0$ . This was confirmed for  $C_2H_4$  (see Fig. 3, showing that **1a** remained at *ca.*  $1.3 \times 10^{-3}$  mol  $dm^{-3}$  or less with only small changes over the course of the reaction). Therefore, on the basis of the steady-state assumption, the ratio  $k_2/k_1$  derived from equation (6) is expressed as in (7). For the case where the alkene is in large

$$k_2/k_1 = [SNS^+]/[\mathbf{1}] = ([SNS^+]_0 - [\mathbf{1}] - [\mathbf{2}])/[\mathbf{1}] \quad (7)$$

excess (in an experiment designed to determine the absolute first rate constant  $k_1$ ),  $[\mathbf{1}] \ll [\mathbf{2}]$  (Fig. 3). Thus substitution of (5) with (7) leads to equation (8), where  $\alpha = [SNS^+]_0 -$

$$-d[\text{alkene}]/dt = k_1[\text{alkene}]([\text{alkene}] + 2\alpha) \quad (8)$$

$\frac{1}{2}[\text{alkene}]_0$ . Integration of (8) with boundary condition  $t = 0$ ,  $[\text{alkene}] = [\text{alkene}]_0$ , leads (see SUP 57125) to equation (9)

$$\ln\{1 + (2\alpha/[\text{alkene}])\} = 2\alpha k_1 t + \ln\{1 + (2\alpha/[\text{alkene}]_0)\} \quad (9)$$

and  $k_1$  can be found from the slope of a plot of  $\ln\{1 + (2\alpha/[\text{alkene}])\}$  versus  $t$  curve.

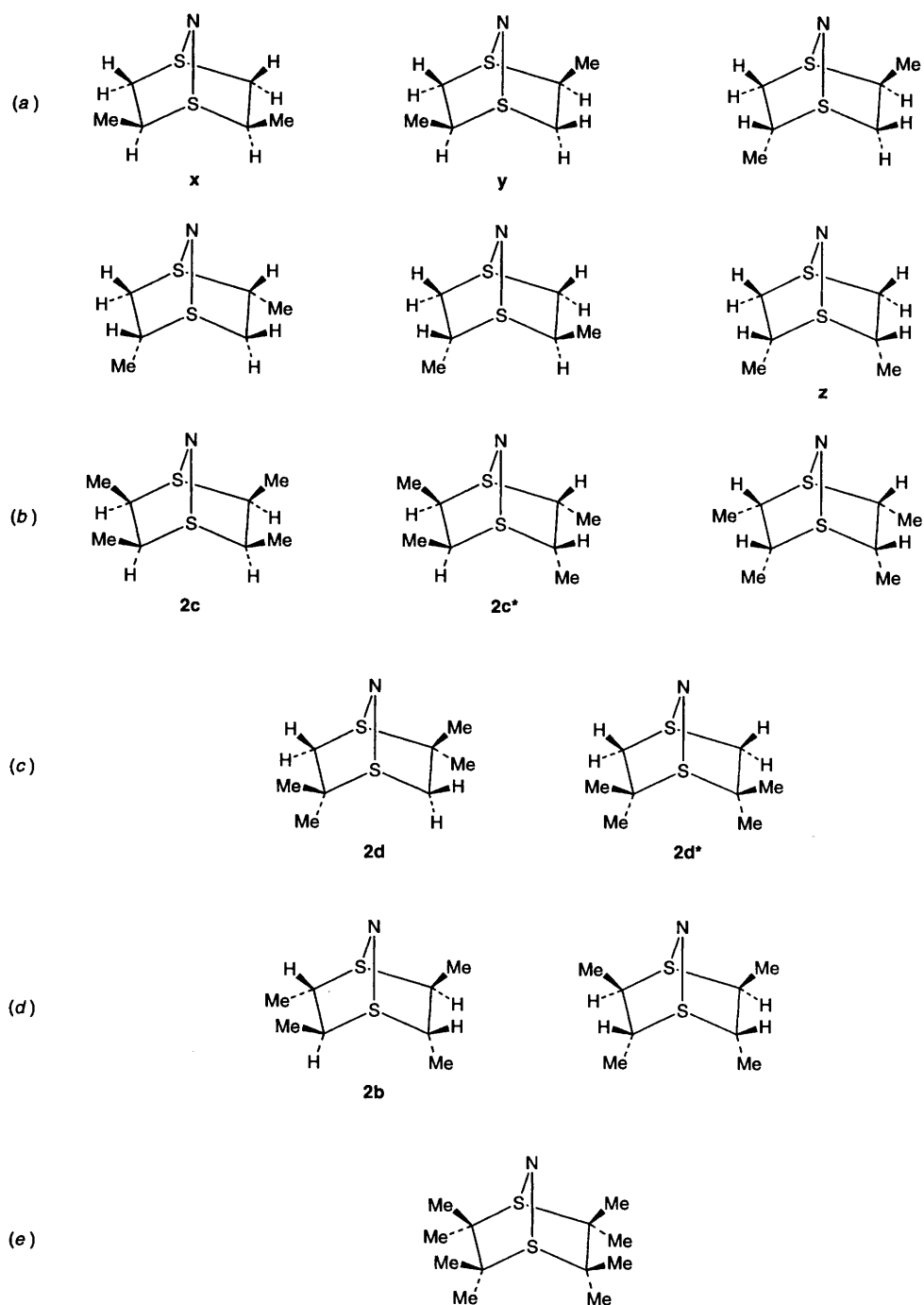


**Fig. 5** Possible isomers of the 1:2 SNS<sup>+</sup> cycloaddition products **2**. Alkene = H<sub>2</sub>CCHMe (a), *cis*-MeHCCHMe (b), H<sub>2</sub>CCMe<sub>2</sub> (c), *trans*-MeHCCHMe (d) and Me<sub>2</sub>CCMe<sub>2</sub> (e)

The reaction of C<sub>2</sub>H<sub>4</sub> with SNS<sup>+</sup> as a function of time was monitored by <sup>1</sup>H NMR spectroscopy. The variation of  $\ln\{1 + (2\alpha/[C_2H_4])\}$  with time [see equation (9)] was linear (slope  $-0.0270\text{ s}^{-1}$ , see Fig. 7), indicating that the reaction is an overall second-order process (first order in [C<sub>2</sub>H<sub>4</sub>] and in [SNS<sup>+</sup>]), consistent with the proposed cycloaddition. The absolute rate constant ( $k_1$ ) of the first cycloaddition was determined from the slope in Fig. 7 to be  $0.190\text{ dm}^3\text{ mol}^{-1}\text{ s}^{-1}$ , 128 times as great as that of the MeCN cycloaddition with SNS<sup>+</sup> ( $1.49 \times 10^{-3}\text{ dm}^3\text{ mol}^{-1}\text{ s}^{-1}$ ). This fits the correlation of the reaction rates to ionization potentials previously established from various nitrile and alkyne reactions (Fig. 8). We also observed that the reaction of *cis*-MeHCCHMe (ionization potential 9.12 eV)<sup>14</sup> proceeds even faster than that of C<sub>2</sub>H<sub>4</sub> (10.5 eV).<sup>15</sup> However, it was too fast to measure the absolute rate constant. That is, the rate of reaction is inversely proportional to the ionization

energy of the alkene (nitrile or alkyne). The dominant interaction in the cycloaddition is between the HOMO of the alkene (donor) and the LUMO of SNS<sup>+</sup> (acceptor) shown in Figs. 6 and 9. We have proposed that the symmetry-allowed cycloadditions of nitriles and alkynes are concerted but asynchronous,<sup>2d</sup> and this applies to the first alkene cycloadditions with SNS<sup>+</sup> because of the similarity of the geometrical features of alkenes to those of alkynes and nitriles, although we cannot rule out a synchronous pathway (see Fig. 9). Calculations of reaction pathways are under current investigation at the University of New Brunswick by Grein and co-workers.<sup>16</sup>

Contrary to expectation [if  $\Delta E_2 > \Delta E_1$  (Fig. 6) the second cycloaddition should be slower than the first] our preliminary experimental results indicated that the second cycloaddition was faster than the first. The absolute rate constant ( $k_2$ ) of the

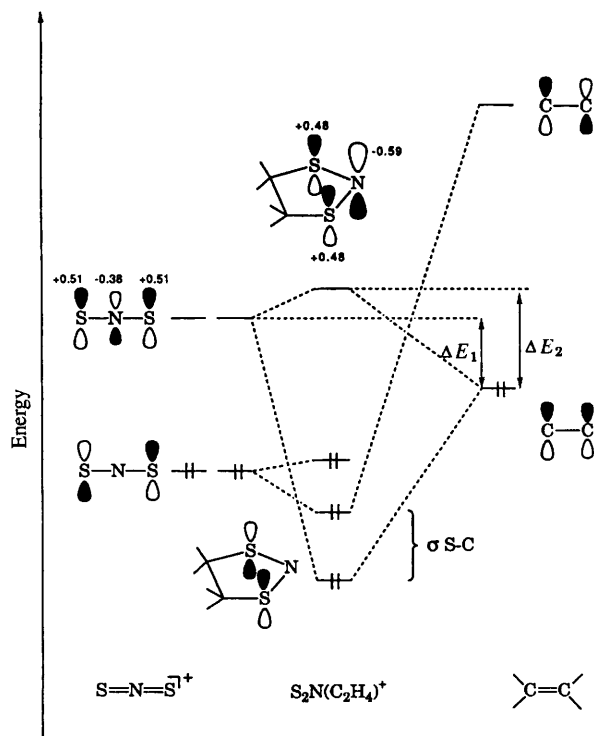


Fig. 6 Energies of the molecular orbitals (STO-3G) of  $\text{SNS}^+$ ,  $\text{C}=\text{C}$  and cation **1a**. The numbers correspond to the corresponding values of the  $P_z$  eigenvector coefficients

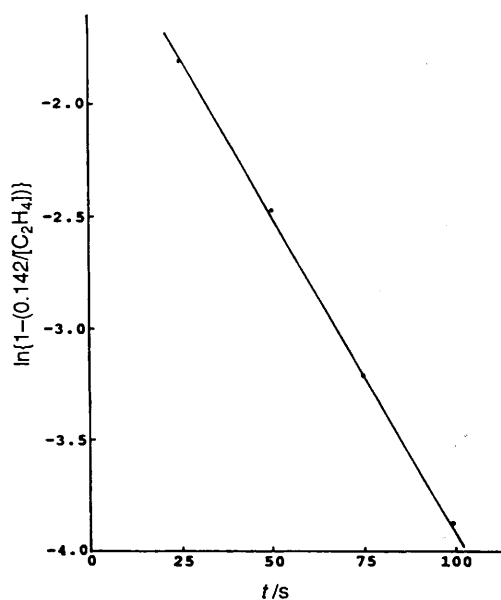


Fig. 7 Plot of  $\ln\{1 - (0.142/[\text{C}_2\text{H}_4])\}$  ( $[\text{C}_2\text{H}_4]$  = concentration of  $\text{C}_2\text{H}_4$  in  $\text{mol dm}^{-3}$ ) versus reaction time for cycloaddition of  $\text{C}_2\text{H}_4$  to  $\text{SNS}^+$

second cycloaddition of ethene with cation **1a** was not precisely determined by the available data. However, the ratio of the rate constant of the second cycloaddition ( $k_2$ ) to that of the first ( $k_1$ ) with  $\text{SNS}^+$ ,  $k_2/k_1$ , was estimated from trial numerical integrations (see SUP 57125) to be in the range  $7 < k_2/k_1 < 20$ , which is in accord with the steady-state assumption. The numerical integration treatment also showed that, although equation (7) does not give an exact value of the  $k_2/k_1$  ratio (since the steady-state approximation is not exact), it can be employed to estimate the lower limit of  $k_2/k_1$  when  $\text{SNS}^+$  is in excess, which for  $\text{C}_2\text{H}_4$  was calculated to be 7.3, consistent with the lowest value of  $k_2/k_1$  obtained by numerical integration. Similarly, the lower limits of  $k_2/k_1$  for the *cis*-MeHCCHMe and

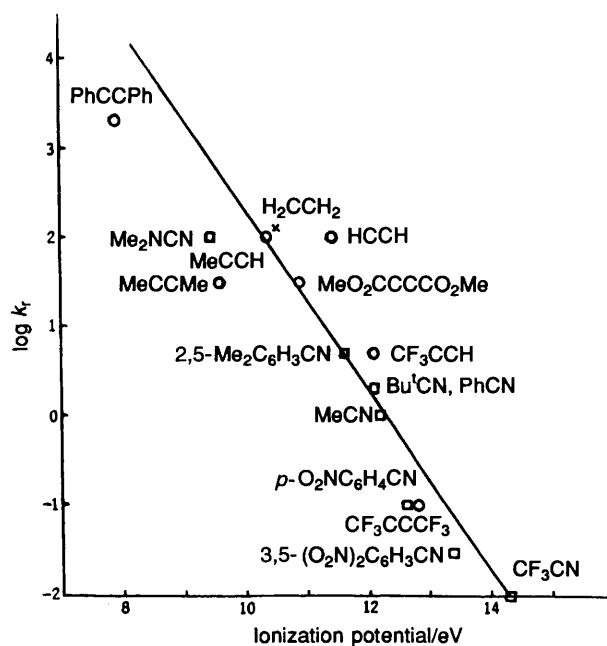


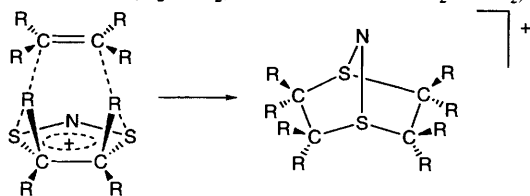
Fig. 8 Plot of the logarithm of relative rate constant of cycloaddition of nitriles ( $\square$ ), alkynes ( $\circ$ ) and ethene ( $\times$ ) against ionization potential (eV). Rates are given relative to MeCN

$\text{H}_2\text{CCMe}_2$  cycloadditions with  $\text{SNS}^+$  were calculated according to equation (7) to be 4.2 and 2.5 respectively. The magnitude of the  $k_2/k_1$  ratio can be affected by many factors. The major influence, however, may be roughly attributed to simple statistical and steric effects as shown in Table 9. For the three alkenes in Table 9 only  $\text{C}_2\text{H}_4$  has 100% fruitful pathways, and the percentages of such pathways for the other two are much lower. In addition, the cycloaddition of  $\text{C}_2\text{H}_4$  involves minimum steric hindrance because it involves  $\text{H}\cdots\text{H}$  interactions. Therefore, both statistical and steric factors favour this cycloaddition over those of the other two alkenes, and it has the largest  $k_2/k_1$  value (7.3). The statistical factor favours the cycloaddition of  $\text{H}_2\text{CCMe}_2$  (50% fruitful pathways) over that of *cis*-MeHCCHMe (25% fruitful pathways). However, the fruitful pathways of the  $\text{H}_2\text{CCMe}_2$  cycloaddition involve sterically unfavourable  $\text{H}\cdots\text{Me}$  interactions, but those of the *cis*-MeHCCHMe cycloaddition only involve  $\text{H}\cdots\text{H}$  interactions. Therefore, the reactions may be dominated by steric effects, resulting in a larger  $k_2/k_1$  value for the *cis*-MeHCCHMe cycloaddition (4.2) than for the  $\text{H}_2\text{CCMe}_2$  reactions (2.5). In contrast to the asynchronous cycloaddition reactions of alkenes with linear  $\text{SNS}^+$ , the cycloaddition reaction of alkene with the first cycloadduct **1** containing an angular SNS moiety probably occurs *via* a concerted, but synchronous pathway as illustrated in Fig. 9. The sulfur atoms are closer together in **2a** than in  $\text{SNS}^+$ , and there are no two nodes intervening as is the case for  $\text{SNS}^+$  (see Fig. 9). This gives more initial overlap than in the asynchronous interaction of the FMOs of  $\text{SNS}^+$  and the alkene, and may account for the faster rate of the second cycloaddition for small, non-sterically hindered alkenes. This mechanism is further supported by the stereospecificity and steric effects observed for the second cycloadditions.\*

#### Generality of the 1:1 and 1:2 cycloadditions of $\text{SNS}^+$ with alkenes and other multiple bonds

A simple thermodynamic analysis based on the energy difference between the bonds formed and the bonds broken in

\* Interestingly, the cycloaddition reactions of alkenes with **3** leading to **4** have been shown to be slow.<sup>29</sup> This may arise in part from back bonding to the sulfur atoms from the chlorines, resulting in a higher LUMO.

**Table 9** 1:2 Cycloadditions of SNS(alkene)<sup>+</sup> with alkene (H<sub>2</sub>CCH<sub>2</sub>, *cis*-MeHCCHMe or H<sub>2</sub>CCMe<sub>2</sub>)

Eight possible pathways of approach for all the alkenes to the sulfur centres

	H <sub>2</sub> CCH <sub>2</sub>	<i>cis</i> -MeHCCHMe	H <sub>2</sub> CCMe <sub>2</sub>
Pathways involving H...H interactions <sup>a</sup>	8	2	0
Pathways involving H...Me interactions <sup>a</sup>	—	4	4
Pathways involving Me...Me interactions <sup>a</sup>	—	2	4
Pathways leading to the observed 1:2 product	8	2	4
Percentage of fruitful pathways	100	25	50
<i>k</i> <sub>2</sub> / <i>k</i> <sub>1</sub> <sup>b</sup>	7.3	4.2	2.5

<sup>a</sup> The interactions may occur between substituent groups (R...R and R...R) in the two reactants during cycloaddition and in the final product in *endo* positions. The H...H interactions do not effect steric hindrance for the cycloadditions. The H...Me interactions may effect partial steric hindrance. The Me...Me interactions make the cycloadditions completely sterically hindered. For the *cis*-MeHCCHMe cycloaddition, although the pathways involving H...Me interactions might not be completely sterically hindered, the reaction would be expected preferably to take the pathways only involving H...H interactions. <sup>b</sup> The magnitude of *k*<sub>2</sub>/*k*<sub>1</sub> may be roughly explained from simple statistical and steric effects. Both factors favour C<sub>2</sub>H<sub>4</sub> cycloaddition. The statistical factor favours H<sub>2</sub>CCMe<sub>2</sub>, however the *cis*-MeHCCHMe cycloaddition involves only H...H interactions, whereas H<sub>2</sub>CCMe<sub>2</sub> cycloadditions necessitate unfavourable Me...H interactions both during the reactions and in the final product (*endo*-Me-*endo*-Me).

the cycloaddition process can be used to estimate the enthalpy change of these cycloaddition reactions.<sup>19</sup> The enthalpy change for this process is estimated (very approximately\*) to be -220 kJ mol<sup>-1</sup>. A similar value of the energy change is obtained for the cycloaddition of cation **1** to a second alkene molecule by using this model. However, the strain of the eclipsed groups within and between the C<sub>2</sub>H<sub>4</sub> fragments is likely to lower the overall energy of **2**. Using a similar approach, the energy changes on cycloadditions of SNS<sup>+</sup> to other unsaturated bonds are estimated (kJ mol<sup>-1</sup>) to be: S=C (-380), S=N (-340), N=S (-330), C=P (-280), C=C (-260), N=N (-230), C=C (-220), P=S (-180), N=P (-140), C=N (-120), C=O (-70) and N=O (-40). If the reactions are concerted and symmetry allowed and not sterically hindered, then it is predicted that their rates would be inversely proportional to their ionization energies as shown

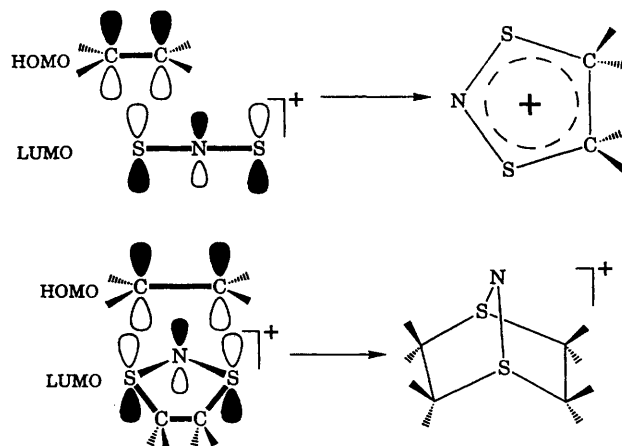


**Fig. 9** Possible FMO interactions for the cycloadditions of alkene (HOMO) to SNS<sup>+</sup> (LUMO) (asynchronous pathway) and to **1** (LUMO) (synchronous pathway)

\* The reaction of SNS<sup>+</sup> with a doubly bonded alkene molecule is modelled as the dissociation of single S-N and C-C π bonds with the formation of two S-C σ bonds. The free-energy change is calculated according to the equation  $\Delta G = \Delta H_f(\text{S=N}, \pi) + \Delta H_f(\text{C=C}, \pi) - 2\Delta H_f(\text{S-C}, \sigma) + K_{\text{deloc}} + \beta$ . Here *K*<sub>deloc</sub> represents the π delocalization energy and β the changes in entropy, charge delocalization, difference in delocalization energy of SNS<sup>+</sup> and the cycloadduct, solvation and/or crystal-lattice energy changes. These terms were neglected on estimation of the free-energy change. The cycloaddition of SNS<sup>+</sup> to a triple bond (e.g. alkynes and nitriles) is assumed to be a similar process and its *K*<sub>deloc</sub> and β values are greater than those for an alkene cycloaddition. Therefore, the cycloadditions of alkynes are thermodynamically more favourable than those of alkenes. Using the total energies of SNS<sup>+</sup> (-849.090 24), C<sub>2</sub>H<sub>4</sub> (-78.031 72), **1a** (-927.207 91) and **2a** (-1005.269 14 E<sub>h</sub>), a value of -226 kJ mol<sup>-1</sup> (all calculations were performed at the RHF/6-31G\* level) was obtained for the formation of **1a** from SNS<sup>+</sup> and C<sub>2</sub>H<sub>4</sub>. This is in good agreement with the estimated -220 kJ mol<sup>-1</sup>. However, the calculated total energies predict the formation of **2a** from **1a** and C<sub>2</sub>H<sub>4</sub> to be endothermic (+83 kJ mol<sup>-1</sup>), whereas the formation of **2a** from SNS<sup>+</sup> and 2 equivalents of C<sub>2</sub>H<sub>4</sub> is predicted to be exothermic (-330 kJ mol<sup>-1</sup>), in agreement with the value estimated using bond-dissociation energies. A higher level of calculation will be needed to obtain consistent results.

in Fig. 8. We have reported that SNS<sup>+</sup> undergoes a rapid reaction with Bu<sup>t</sup>C≡P<sup>2h</sup> consistent with its low ionization energy (9.70 eV). Banister *et al.*<sup>2f</sup> have reported that SNS<sup>+</sup> cycloadds to N=N. In contrast, the cycloaddition of SNS<sup>+</sup> with Me<sub>2</sub>CO (ionization potential 9.69 eV)<sup>17</sup> and Bu<sup>t</sup><sub>2</sub>CO (ionization potential presumably lower) did not occur,<sup>2g</sup> implying that the reactions may in fact be thermodynamically unfavourable under ambient conditions (*i.e.* β may be greater than +70 kJ mol<sup>-1</sup>, see footnote\*). Based on the above considerations, cycloaddition reactions of SNS<sup>+</sup> with a wide variety of simple unsaturated centres can be anticipated under ambient or mild conditions.

## Conclusion

We have previously shown that SNS<sup>+</sup> (as the AsF<sub>6</sub><sup>-</sup> salt) undergoes a general quantitative concerted symmetry-allowed

cycloaddition reaction with a variety of nitriles, alkynes and  $\text{SN}^+$ .<sup>2</sup> In this work, we establish that  $\text{SNS}^+$  also undergoes similar cycloadditions with alkenes to give  $\text{AsF}_6^-$  salts of the cations **1**, likely fluxional, which undergo a second concerted symmetry-allowed cycloaddition reaction with a second alkene molecule to give  $\text{AsF}_6^-$  salts containing the norbornane-like cations **2**, the crystal structure of which has been determined for **2a**.<sup>6</sup> The purity of both types of cycloadducts was established by chemical analyses and IR and NMR spectroscopies. The second cycloaddition reactions are under steric control, and they are stereospecific for  $\text{H}_2\text{CCMe}_2$ , *cis*- and *trans*- $\text{MeHCCHMe}$  and do not occur for  $\text{Me}_2\text{CCMe}_2$ . This work provides general routes to cations **1** and with some steric restrictions to cations **2**, both classes being unknown prior to this work.

The rate of the cycloaddition of  $\text{SNS}^+$  to  $\text{C}_2\text{H}_4$  was first order in the concentrations of both reagents and the absolute rate constant compared well with those for the  $\text{C}\equiv\text{C}$  and  $\text{C}\equiv\text{N}$  cycloadditions. The rate of reaction of *cis*- $\text{MeHCCHMe}$  was faster than that of  $\text{C}_2\text{H}_4$  consistent with its lower ionization potential. We can reasonably conclude that reaction rates with  $\text{SNS}^+$  are approximately proportional to the reciprocal of the ionization potential of the multiply bonded substrates for the three types of multiple bonds, and that all three are concerted symmetry-allowed cycloaddition reactions of the reverse-electron-demand type, *i.e.* in the context of a simple FMO model<sup>18</sup> the reactions proceed *via* the interaction between the HOMO of the multiple bond (donor) and the LUMO of  $\text{SNS}^+$  (acceptor), and are electronically controlled. We predict that a large number of unsaturated centres connecting X and Y will undergo symmetry-allowed cycloaddition reactions with  $\text{SNS}^+$  and that the rate of reaction will be proportional to the reciprocal of the ionization potential (reactant containing XY) with some steric effects if large groups are appended to XY. A simple bond made–bond broken model is proposed to estimate whether or not the cycloaddition is thermodynamically allowed.

The cycloaddition of alkenes to cation **1** is faster than to  $\text{SNS}^+$  for small R, but strongly influenced by the steric activity of R. The lower limits of the relative rates of this cycloaddition to the first cycloaddition of alkene with  $\text{SNS}^+$  are estimated to be approximately 7.3, 4.2 and 2.5 for  $\text{H}_2\text{CCH}_2$ , *cis*- $\text{MeHCCHMe}$  and  $\text{H}_2\text{CCMe}_2$  respectively and no second cycloaddition is observed for  $\text{Me}_2\text{CCMe}_2$ . The bent geometry of the  $\text{SNS}$  fragment in the  $\text{R}_2\text{CSNSCR}_2^+$  cation, allowing good symmetrical overlap of its  $\text{SNS}^+$ -like LUMO and the HOMO of the alkene, as well as the effect of the steric nature of R on the relative reaction rates, suggest that the cycloaddition occurs *via* a reverse-electron demand, concerted symmetry-allowed, synchronous pathway. The concerted synchronous pathway of the second cycloaddition gives greater overlap of frontier orbitals than those of  $\text{SNS}^+$  and alkene occurring in the first cycloaddition either *via* a concerted synchronous, or (more likely) concerted asynchronous pathway, accounting for the generally faster rate of the second cycloaddition.

## Acknowledgements

We thank Dr. L. Calhoun for assistance with NMR spectroscopy, and the Atlantic NMR Centre of Dalhousie University for obtaining the 360 MHz NMR spectra. We also thank the Natural Sciences and Engineering Research Council (Canada) for funding and for graduate scholarships (to S. B. and M. J. S.).

## References

- 1 S. Parsons and J. Passmore, *Acc. Chem. Res.*, 1994, **27**, 101 and refs. therein.
- 2 (a) G. K. MacLean, J. Passmore, M. N. S. Rao, M. J. Schriver, P. S. White, D. Bethell, R. S. Pilkington and L. H. Sutcliffe, *J. Chem.*

- Soc.*, *Dalton Trans.*, 1985, 1405; (b) G. K. MacLean, J. Passmore, M. J. Schriver, P. S. White, D. Bethell, R. S. Pilkington and L. H. Sutcliffe, *J. Chem. Soc., Chem. Commun.*, 1983, 807; (c) J. Passmore and M. J. Schriver, *Inorg. Chem.*, 1988, **27**, 2749; (d) S. Parsons, J. Passmore, M. J. Schriver and P. S. White, *J. Chem. Soc., Chem. Commun.*, 1991, 369; S. Parsons, J. Passmore, M. J. Schriver and X. Sun, *Inorg. Chem.*, 1991, **30**, 3342; (e) J. Passmore, X. Sun and S. Parsons, *Can. J. Chem.*, 1992, **70**, 2972; (f) A. J. Banister, I. Lavender, S. E. Lawrence, J. M. Rawson and W. J. Clegg, *J. Chem. Soc., Chem. Commun.*, 1994, 29; (g) M. J. Schriver, Ph.D. Thesis, University of New Brunswick, 1989; (h) S. Parsons, J. Passmore and X. Sun, *Phosphorus Sulfur Silicon Relat. Elem.*, 1994, **93/94**, 435; S. Parsons, J. Passmore, X. Sun and M. Regitz, *Can. J. Chem.*, 1995, **73**, 1312; (i) X. Sun, Ph.D. Thesis, University of New Brunswick, 1995; (j) J. Jacobs, S. E. Ulic, H. Willner, G. Schatte, J. Passmore, S. V. Sereda and T. S. Cameron, *J. Chem. Soc., Dalton Trans.*, 1996, 383.
- 3 S. W. Liblong, R. T. Oakley, A. W. Cordes and M. C. Noble, *Can. J. Chem.*, 1983, **61**, 2062.
- 4 S. Mataka, K. Takahashi, Y. Yamada and M. Tashiro, *J. Heterocycl. Chem.*, 1979, **16**, 1009; S. T. A. K. Daley, C. W. Rees and D. J. Williams, *J. Chem. Soc., Chem. Commun.*, 1984, 55; J. L. Morris and C. W. Rees, *Chem. Soc. Rev.*, 1986, **15**, 1 and refs. therein.
- 5 R. T. Boeré, J. A. Eng, K. Preuss, M. Parvez, C. D. Bryan and A. W. Cordes, *Can. J. Chem.*, 1994, **72**, 1171.
- 6 N. Burford, J. P. Johnson, J. Passmore, M. J. Schriver and P. S. White, *J. Chem. Soc., Chem. Commun.*, 1986, 966.
- 7 M. P. Murchie and J. Passmore, *Inorg. Synth.*, 1986, **24**, 76; M. P. Murchie, R. Kapoor, J. Passmore and G. Schatte, *Inorg. Synth.*, 1996, **31**, in the press.
- 8 E. G. Awere and J. Passmore, *J. Chem. Soc., Dalton Trans.*, 1992, 1343.
- 9 L. Cassidei and O. Sciacovelli, *QCPE Bull.*, 1983, **3**, 45.
- 10 W. H. Mueller and M. Dines, *J. Heterocycl. Chem.*, 1969, **6**, 677 and refs. therein.
- 11 A. Appleby, T. Chivers, A. W. Cordes and R. Vollmerhaus, *Inorg. Chem.*, 1991, **30**, 1392.
- 12 (a) GAUSSIAN 92/DFT, Revision G.3, M. J. Frisch, G. W. Trucks, H. B. Schlegel, P. M. W. Gill, B. G. Johnson, M. W. Wong, J. B. Foresman, M. A. Robb, M. Head-Gordon, E. S. Replogle, R. Gomperts, J. L. Andres, K. Raghavachari, J. S. Binkley, C. Gonzalez, R. L. Martin, D. J. Fox, D. J. Defrees, J. Baker, J. J. P. Stewart and J. A. Pople, Gaussian Inc., Pittsburgh, PA, 1993; (b) J. B. Foresman and A. Frisch, *Exploring Chemistry with Electronic Structure Methods: A Guide to Using Gaussian*, Gaussian Inc., Pittsburgh, PA, 1993; (c) O. Glemser, E. Kindler, B. Krebs, R. Mews, F. M. Schnepel and J. Wegener, *Z. Naturforsch., Teil B*, 1980, **35**, 657; (d) A. M. Griffin and G. M. Sheldrick, *Acta Crystallogr., Sect. B*, 1975, **31**, 893; (e) A. J. Banister, I. B. Gorrell and R. S. Roberts, *J. Chem. Soc., Faraday Trans. 2*, 1985, 1783; (f) L. Pauling, *The Nature of the Chemical Bond*, 3rd edn., Cornell University Press, Ithaca, NY, 1960, p. 239; (g) S. C. Nyburg, *J. Cryst. Mol. Struct.*, 1973, **3**, 331; (h) A. J. Banister, J. A. Durrant and I. B. Gorrell, *J. Chem. Soc., Faraday Trans. 2*, 1985, 1771; (i) W. V. F. Brooks, T. S. Cameron, S. Parsons, J. Passmore and M. J. Schriver, *Inorg. Chem.*, 1994, **33**, 6230.
- 13 (a) S. Parsons, J. Passmore, M. J. Schriver and P. S. White, *Can. J. Chem.*, 1990, **68**, 852, and refs. therein; (b) J. Mason, *Chem. Rev.*, 1981, **81**, 205; (c) T. Chivers, *Chem. Rev.*, 1985, **85**, 341; *Acc. Chem. Res.*, 1984, **17**, 166; (d) T. C. Shields and A. N. Kuota, *J. Am. Chem. Soc.*, 1969, **91**, 5415; J. Emsley, D. W. Griffiths and G. J. J. Jayne, *J. Chem. Soc., Perkin Trans. 1*, 1979, 228; (e) J. Emsley, D. W. Griffiths and R. Osborn, *J. Chem. Soc., Chem. Commun.*, 1978, 658; (f) D. H. R. Barton and W. Doering, (Editors), *Applications of Nuclear Magnetic Resonance Spectroscopy in Organic Chemistry*, Pergamon, Oxford, 1969.
- 14 K. Watanabe, T. Nakayama and J. Mottl, *J. Quant. Spectrosc. Radiat. Transfer*, 1962, **2**, 369.
- 15 R. Botter, V. H. Dibeler, J. A. Walker and H. M. Rosenstock, *J. Chem. Phys.*, 1966, **45**, 1298.
- 16 F. Grein, personal communication; M. Sannigrahi, M.Sc. Thesis, University of New Brunswick, 1994.
- 17 K. Watanabe, *J. Chem. Phys.*, 1954, **22**, 1564.
- 18 R. B. Woodward and P. Hoffmann, *The Conservation of Orbital Symmetry*, Academic Press, New York, 1970.

Received 11th August 1995; Paper 5/05408G